

AD _____

GRANT NUMBER: DAMD17-94-J-4048

TITLE: Rotational Resonance NMR Structural Studies of the neu
Receptor Transmembrane Domain

PRINCIPAL INVESTIGATOR: Steven O. Smith, Ph.D.

CONTRACTING ORGANIZATION: Yale University
New Haven, CT 06520-8047

REPORT DATE: July 1996

TYPE OF REPORT: Final

19960919 024

PREPARED FOR: Commander
U.S. Army Medical Research and Materiel Command
Fort Detrick, Frederick, Maryland 21702-5012

DISTRIBUTION STATEMENT: Approved for public release;
distribution unlimited

The views, opinions and/or findings contained in this report are those of the author(s) and should not be construed as an official Department of the Army position, policy or decision unless so designated by other documentation.

DTIC QUALITY INSPECTED 1

REPORT DOCUMENTATION PAGE

Form Approved

OMB No. 0704-0188

Public reporting burden for this collection of information is estimated to average 1 hour per response, including the time for reviewing instructions, searching existing data sources, gathering and maintaining the data needed, and completing and reviewing the collection of information. Send comments regarding this burden estimate or any other aspect of this collection of information, including suggestions for reducing this burden, to Washington Headquarters Services, Directorate for Information Operations and Reports, 1215 Jefferson Davis Highway, Suite 1204, Arlington, VA 22202-4302, and to the Office of Management and Budget, Paperwork Reduction Project (0704-0188), Washington, DC 20503.

1. AGENCY USE ONLY (Leave blank)		2. REPORT DATE July 1996	3. REPORT TYPE AND DATES COVERED Final (23 May 94 - 23 Jun 96)	
4. TITLE AND SUBTITLE Rotational Resonance NMR Structural Studies of the neu Receptor Transmembrane Domain			5. FUNDING NUMBERS DAMD17-94-J-4048	
6. AUTHOR(S) Steven O. Smith, Ph.D.				
7. PERFORMING ORGANIZATION NAME(S) AND ADDRESS(ES) Yale University New Haven, CT 06520-8047			8. PERFORMING ORGANIZATION REPORT NUMBER	
9. SPONSORING/MONITORING AGENCY NAME(S) AND ADDRESS(ES) Commander U.S. Army Medical Research and Materiel Command Fort Detrick, MD 21702-5012			10. SPONSORING/MONITORING AGENCY REPORT NUMBER	
11. SUPPLEMENTARY NOTES				
12a. DISTRIBUTION / AVAILABILITY STATEMENT Approved for public release; distribution unlimited			12b. DISTRIBUTION CODE	
13. ABSTRACT (Maximum 200) The objective of this Exploratory Award was to establish whether magic angle spinning NMR and polarized infrared spectroscopy could be applied to obtain high resolution structural constraints on the transmembrane domain of the neu/erbB-2 receptor in membrane environments. Such data would be able to address specific models for receptor activation by the transforming glutamic acid 664 mutation. The ultimate goal has been to obtain a high resolution 3D structure of the transmembrane domain of the constitutively activated receptor that can be used to establish the activation mechanism and possibly serve as a guide to the design of competitive inhibitors. The results obtained to date demonstrate that the approach outlined was successful and has provided the ground work for further studies. The major conclusion that can be drawn thus far is that the valine to glutamic acid mutation that activates the neu receptor, and is associated with a large number of breast cancers, functions by stabilizing receptor dimers via strong head-to-head hydrogen bonding interactions of the protonated glutamic acid COOH side chain.				
14. SUBJECT TERMS Breast Cancer			15. NUMBER OF PAGES 38	
			16. PRICE CODE	
17. SECURITY CLASSIFICATION OF REPORT Unclassified	18. SECURITY CLASSIFICATION OF THIS PAGE Unclassified	19. SECURITY CLASSIFICATION OF ABSTRACT Unclassified	20. LIMITATION OF ABSTRACT Unlimited	

FOREWORD

Opinions, interpretations, conclusions and recommendations are those of the author and are not necessarily endorsed by the US Army.

____ Where copyrighted material is quoted, permission has been obtained to use such material.

____ Where material from documents designated for limited distribution is quoted, permission has been obtained to use the material.

____ Citations of commercial organizations and trade names in this report do not constitute an official Department of Army endorsement or approval of the products or services of these organizations.

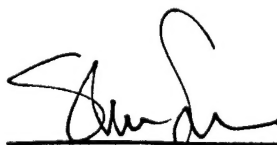
____ In conducting research using animals, the investigator(s) adhered to the "Guide for the Care and Use of Laboratory Animals," prepared by the Committee on Care and Use of Laboratory Animals of the Institute of Laboratory Resources, National Research Council (NIH Publication No. 86-23, Revised 1985).

____ For the protection of human subjects, the investigator(s) adhered to policies of applicable Federal Law 45 CFR 46.

____ In conducting research utilizing recombinant DNA technology, the investigator(s) adhered to current guidelines promulgated by the National Institutes of Health.

____ In the conduct of research utilizing recombinant DNA, the investigator(s) adhered to the NIH Guidelines for Research Involving Recombinant DNA Molecules.

____ In the conduct of research involving hazardous organisms, the investigator(s) adhered to the CDC-NIH Guide for Biosafety in Microbiological and Biomedical Laboratories.



PI - Signature

July 17, 1996

Date

TABLE OF CONTENTS

Rotational Resonance NMR Structural Studies of the neu Receptor Transmembrane Domain

Introduction	2
Body	4
Conclusions	21
References	22
Bibliography of Publications	25
Personnel	25

INTRODUCTION

The *neu/erbB-2* gene encodes a 185 kD receptor tyrosine kinase that is involved in signal transduction across cell membranes [1-3]. The receptor is part of the *erbB* family of receptor tyrosine kinases; it has two cysteine-rich extracellular domains, a single helical membrane-spanning domain and an intracellular tyrosine kinase (TK) domain. Ligand-binding to the extracellular domain activates the TK domain through receptor dimerization. Constitutive activation of the receptor is known to occur by gene overexpression or by a single mutation within the hydrophobic transmembrane sequence where a naturally-occurring valine residue at position 664 is replaced by glutamic acid [1-4]. The point mutation was the first occurrence of an activating mutation in the transmembrane domain of a growth factor receptor and suggested that the structure of the transmembrane domain plays a larger role in the signal transduction process than previously thought.

Two models have been proposed for how the Val 664 → Glu 664 substitution causes cell trans-formation. The first involves a change in the secondary structure of the transmembrane (TM) domain. Brandt-Rauf et al. (1990) [5] calculated that the minimum-energy conformation in the region of Val 664 contains a sharp bend at positions 664 and 665, while the transforming sequence exists as an α -helix. The second model is that the glutamate side chain promotes dimerization via hydrogen-bonding interactions [6]. In this case, the helices are thought to be held in the "active" state by hydrogen bonding between the Glu 664 carboxylic acid side chain on one helix and the Glu 664 side chain or peptide backbone carbonyl and amide groups of the second helix. Consistent with this model, the transforming protein (with a glutamic acid residue at position, Glu 664) has a higher propensity to form dimers than the normal (Val 664) protein [7]. The position of the glutamic acid residue is sequence specific. Bargmann and Weinberg originally demonstrated that substitution of glutamic acid at positions 663 or 665 did not activate the receptor [1].

Stern and coworkers have undertaken an extensive mutagenesis study of the TM domain of *neu* to define the residues that are responsible for receptor activation [4]. They found that a sub-domain, -V₆₆₃- E₆₆₄ -G₆₆₅-, is important. The domain differs slightly from that predicted by Sternberg and Gullick [6], most notably in the importance of A₆₆₁ for receptor dimerization. Gullick and coworkers [8] have shown that intracellular expression of small proteins, corresponding to the TM and membrane-proximal domains of *neu* and containing variations on the activated *neu* TM sequence, inhibits growth of *neu* transformed cells. However, a simple model involving hydrogen-bonding interactions of the Glu 664 may not be sufficient to explain receptor activation. Stern and coworkers [4] have shown, by moving the VEG sub-domain around in the TM sequence and by generating mutants that dimerize without activating the receptor, that dimerization alone is insufficient to cause cell transformation and that the interactions are likely to be highly specific. No direct evidence has been obtained for the points of contact in the receptor dimers and a high-resolution structure is needed to determine the exact nature of the protein interactions and whether they are distributed along the length of the TM domain.

In order to determine the structure of the transmembrane domain of the *neu/erbB-2* receptor and address the molecular mechanism of receptor activation by the transforming Val 664 to Glu 664 mutation, magic angle spinning (MAS) NMR and polarized Fourier transform infrared (FTIR) studies have been undertaken. We have previously shown that MAS NMR and FTIR measurements provide a feasible approach for structural studies on membrane proteins [9-11].

MAS yields high resolution NMR spectra of membrane proteins in bilayer environments [6] and several different strategies have been developed for measuring weak dipolar couplings in MAS experiments [12-15]. Of importance for structural studies is that accurate internuclear distances can be derived from measurements of dipolar couplings which in turn provide constraints for generating and evaluating structural models. The two best established approaches are rotational resonance (RR) and rotational echo double resonance (REDOR) NMR. The RR NMR approach selectively restores the dipolar couplings by spinning the sample such that an integral multiple of the MAS frequency is equal to the chemical shift difference ($\Delta\omega$) between two NMR resonances [16-18]. The distance limits for $^{13}\text{C}\dots^{13}\text{C}$ measurements using RR NMR is ~ 6.5 Å with resolution on the order of 0.3 Å. The REDOR NMR approach has been developed to measure weak heteronuclear dipolar couplings, such as those between ^{31}P and ^{13}C or ^{15}N and ^{13}C [19,20]. REDOR relies on the dephasing of magnetization of the observed spin through coupling to a second spin. The distance limit for $^{13}\text{C}\dots^{15}\text{N}$ measurements using REDOR NMR is ~ 5 Å with resolution on the order of 0.2 Å.

The global secondary structure and orientation of membrane proteins and peptides can be probed by polarized FTIR spectroscopy using the amide I vibration as a structurally sensitive marker [21]. The frequency of the amide I mode depends on hydrogen-bonding of the C=O group as well as on the geometry of the peptide backbone. Bands centered at ~ 1654 cm^{-1} correspond to α -helical structures, while bands centered at $1624 - 1637$ cm^{-1} and 1675 cm^{-1} correspond to the out-of-phase and in-phase modes of β -sheet structures, respectively or alternatively β -turn. Fourier self deconvolution (FSD) of the amide I region [22] can yield quantitative estimates of the relative ratios between the different secondary structural elements of the protein [23]. The orientation of C=O group, which dominates the amide I vibration, can be derived from the relative absorption of IR light polarized parallel or perpendicular to the C=O transition dipole moment. Maximum absorption occurs when the polarization of light is parallel to the transition moment. In an α -helix, the C=O transition dipole is known to be oriented at an angle of $\sim 39^\circ$ relative to the helix axis [24-26].

In the first year of this Exploratory Award, we have used both MAS NMR and FTIR to study peptides 38 residues in length that incorporate the transmembrane domain of the activated receptor (neu*TM) or the normal receptor (neuTM). The neuTM and neu*TM nomenclature will be used throughout this report. We have demonstrated that these peptides form extended helical structures oriented perpendicular to the membrane surface when reconstituted into membrane bilayers. Furthermore, the pKa of the Glu 664 carboxyl group in neu*TM in membranes is considerably higher than that of free glutamate indicating the Glu 664 carboxyl group is buried in the membrane interior, possibly in the dimer interface between TM domains.

In the second year, we have applied both NMR and FTIR methods to establish high resolution constraints on the three dimensional structure of the neuTM and neu*TM domains in membrane bilayers. We show that the transmembrane helices pack together in a dimeric structure, most likely in a left-handed coiled coil geometry. These exploratory studies have largely worked and have provided the first detailed high resolution structural data on the molecular interactions responsible for activation of the neu/erbB-2 receptor by the Val to Glu mutation at position 664 in the receptor's transmembrane domain.

BODY

Experimental Methods

*Synthesis and Reconstitution of neuTM and neu*TM.* The neuTM and neu*TM peptides were synthesized using solid-phase methods at the Keck Peptide Synthesis Facility at Yale University. The sequence of the 38-residue peptides corresponds to residues 649-686 in the human neu receptor protein. The sequence of neu*TM is shown below.

AEQRASPVTFIIATV-E664-GVLLFLALVVVVGILIKRRRYK

The lyophilized peptide was dissolved in trifluoroacetic acid and purified using a 5 ml POROS-R1 reverse phase high performance liquid chromatography (RP-HPLC) column (Perceptive Biosystems, Cambridge, MA) equilibrated with 95% H₂O, 2% acetonitrile and 3% 2-propanol. Peptide elution was achieved with a linear gradient to a final solvent composition of 5% H₂O, 38% acetonitrile and 57% 2-propanol. All solvents contained 0.1% trifluoroacetic acid. Fractions containing peptides were then lyophilized and assessed for purity by amino acid analysis (correlation coefficients of > 0.95) and mass spectrometry.

Peptide fractions were lyophilized and reconstituted into lipids as follows. Peptide and lipids were codissolved at a 30:1 molar ratio with 2% n-octyl β -glucopyranoside (Sigma, St. Louis, MO) in trifluoroethanol. Lipids (Avanti Polar Lipids, Alabaster, AL) used were dimyristoyl phosphatidylcholine (DMPC), dimyristoyl phosphatidylserine (DMPS) and dipalmitoyl phosphatidylcholine (DPPC). Samples were dried with nitrogen gas and resolubilized in 6 ml of dialysis buffer [0.5 mM sodium azide, 0.5 mM HEPES, pH 7.0]. For the pH titration studies, samples were split into three dialysis groups for each pH. One of each lipid sample was placed into each of the following buffers: 1 mM MES, 0.5 mM sodium azide, pH 5.5; 1mM HEPES, 0.5 mM sodium azide, pH 7.0; and 1 mM TAPS, 0.5 mM sodium azide, pH 8.5; and dialysed overnight. 300 μ l of each sample were allocated for ATR-FTIR, approximately 100 μ l used for transmission IR, and the remaining pelleted and prepared for MAS-NMR experiments.

Fourier Transform Infrared Spectroscopy. FTIR spectra were recorded on a Nicolet Magna 550 spectrometer purged with N₂ (Madison, WI) and equipped with a MCT/A detector. For transmission spectra, typically 50 μ l of sample (protein concentration of 36 - 90 mM) is dried on AgCl windows with dry air. For polarized ATR-FTIR spectra, the spectrometer was equipped with a KRS-5 wire grid polarizer (0.25 mm spacing, Grasbey Specac, Kent, UK). The sample (~300 μ l, 36 - 90 mM) was dried on the surface of a Ge internal reflection element and placed in a variable angle ATR accessory (Grasbey Specac, Kent, UK). Fourier self deconvolution spectra [FSD, 22] were obtained using a bandwidth of 13 cm⁻¹ and an enhancement factor of 2.4, determined by Byler and Susi [23] to best fit experimental data. The helical content and orientation was determined using the approach described in our recent work on phospholamban [9].

For the SH exchange measurements, samples (400 μ l) containing 4 mg of dipalmitoylphosphatidylcholine (DPPC) and 0.4 mg of protein in a buffer of 0.1 mM Na₂PO₄ pH 6.8 were centrifuged for 1 h in an A-95 rotor at 178,000g using an airfuge ultracentrifuge (Beckman, Palo Alto, CA). Pellets were resuspended in 75 μ l of either H₂O or D₂O and dried down on germanium IR windows following the procedure of Arkin et al. [31].

Circular Dichroism Spectroscopy. CD spectra were obtained on an AVIV 62DS spectrometer in a quartz cuvette of 0.1 mm pathlength. Repetitive scans were recorded at 28 °C with a 1 s integration time, a 0.5 nm step size and a 1.5 nm bandwidth. The protein concentration in the CD samples was determined to within 10% by amino acid analysis using two aliquots of each sample. Spectra of peptide-free lipid vesicles prepared in parallel with the lipid-peptide samples were used to correct for background lipid absorbance and scattering.

Magic Angle Spinning NMR Spectroscopy. Magic angle spinning NMR experiments were performed on a Chemagnetics CMX 360 MHz spectrometer using a 5 mm high speed double resonance probe from Doty Scientific (Columbia, SC). The sample spinning speed for the rotational resonance experiments was kept constant to within 5 Hz using a spinning speed controller from Doty Scientific. The temperature was maintained at ca. +5°C or -50°C in order to slow residual rotational diffusion of the peptide which might otherwise average the dipolar couplings being measured. The pulse sequence used for the RR NMR experiments has been described previously [32]. Briefly, the sequence begins with ^1H - ^{13}C cross polarization to generate ^{13}C polarization that is then stored on the Z axis with a ^{13}C flip-back pulse. One of the two ^{13}C resonances is selectively inverted with a low power 500 μsec pulse and magnetization is allowed to exchange between the two sites for a variable mixing period (t_m). The power level of the inversion pulse is carefully adjusted to yield the maximum inversion. The distribution of ^{13}C signal at the end of the mix period is detected with a 90° pulse that flips the magnetization into the transverse plane for acquisition of the NMR signal. Strong ^1H decoupling is essential during the variable mix and acquisition periods. The decoupling power was set to a field strength of 83 kHz during the variable delay and acquisition. This level of decoupling was sufficient to maximize RR exchange as determined by a comparison of exchange rates at different decoupling field strengths. Conventional single amplitude CP was replaced by variable amplitude cross polarization (VACP) for these experiments to enhance the carbon signals at high MAS frequencies and yield more reliable intensities [32]. During the 5 msec CP contact time, the ^{13}C amplitude corresponded to a constant spin-lock frequency of ~70 kHz, while the proton amplitude was varied in nine steps each 555 msec in length. The first proton amplitude was centered at a B_1 field strength of 70 kHz and the additional amplitudes were increased or decreased in ~2 kHz steps. The VACP sequence yields stable and reproducible signals that are essential for generating the difference spectra and the magnetization exchange curves used for determining internuclear distances.

Molecular Dynamics Simulations and Energy Minimization. Molecular dynamics and energy minimization procedures were used to generate structural models of neuTM and neu*TM. Hydrogen atoms were introduced using the CHARMM22 parameter set with electrostatic and van der Waals energy terms enabled using the program X-PLOR in order to insure energetically reasonable initial positions for the hydrogen atoms. The model was subsequently subjected to 1000 steps of Powell energy minimization.

Electrostatic calculations were carried out using the program DELPHI (QDIFF) that solves the non-linear Poisson-Boltzmann (P-B) equation. The linear part of the P-B equation was solved using 2000 iterations, while 3000 iterations were used to solve the non-linear portion of the equation. This number of iterations was found to be sufficient for convergence. The only other parameter that was different from default values was the outer dielectric constant which was set to 2.0. Charges were taken from the CHARMM22 all atom parameter set.

Results and Discussion

The results and discussion are broken down according to the Statement of Work outlined in the original Exploratory Award proposal.

Task 1. Determine the secondary structure of the neuTM and neu*TM peptides in bilayers.

- a. Circular dichroism (CD) and FTIR studies will be used to characterize the global secondary structure and assay the reconstitution protocols for the neuTM and neu*TM peptides.
- b. Rotational resonance NMR measurements will be made between Ala 661 (1-¹³C) and Gly 665 (2-¹³C) in the neuTM and neu*TM peptides to establish the local secondary structure.

Task 2. Determine the protonation state and the relative solvent accessibility of Glu 664.

- a. Magic angle spinning NMR measurements will be made on neu*TM (5-¹³C) as a function of pH to establish the protonation state and pK_a of the Glu 664 side chain carboxyl group.
- b. Amide exchange measurements will be made on Val 663 (¹⁵N) to determine the relative solvent accessibility in the neuTM and neu*TM peptides.

Task 3. Determine the three dimensional structure and molecular interactions in the region of Glu 664 in neu*TM.

- a. Interhelical rotational resonance NMR exchange rates will be measured to establish contacts between Glu 664 and sites across the dimer interface.
- b. Interhelical REDOR NMR dephasing rates will be measured to establish contacts between Gln 664 and sites across the dimer interface.
- c. Molecular dynamics and energy minimization procedures will be used to obtain a 3D structure of neu*TM consistent with the NMR and FTIR structural constraints.

Task 1a: CD and FTIR Studies of neuTM and neu*TM

We first investigated the global secondary structure of the neu (Val 664) transmembrane sequence. The neu peptide incorporated into DMPC bilayers at pH 7.0 is almost entirely helical. The amide I band is observed at 1655 cm⁻¹ in polarized attenuated total reflection (ATR) -FTIR spectra (Figure 1). This frequency is characteristic of helical secondary structure. Fourier self-deconvolution (FSD) enhances the resolution of the frequency components in the amide I envelope [22] and clearly shows the absence of other secondary structural elements. The residual intensity observed in the FSD spectrum (~15% of the total intensity) can in large part be attributed to the side chain vibrations of arginine, lysine and glutamine residues present in the neu transmembrane sequence. There are 4 arginines, 2 lysines and 1 glutamine in the transmembrane neu peptides which are estimated to represent ~11% of the total intensity between 1600 and 1700 cm⁻¹ based on the bandwidths and extinction coefficients previously reported for amino acid side chain and peptide backbone vibrations.

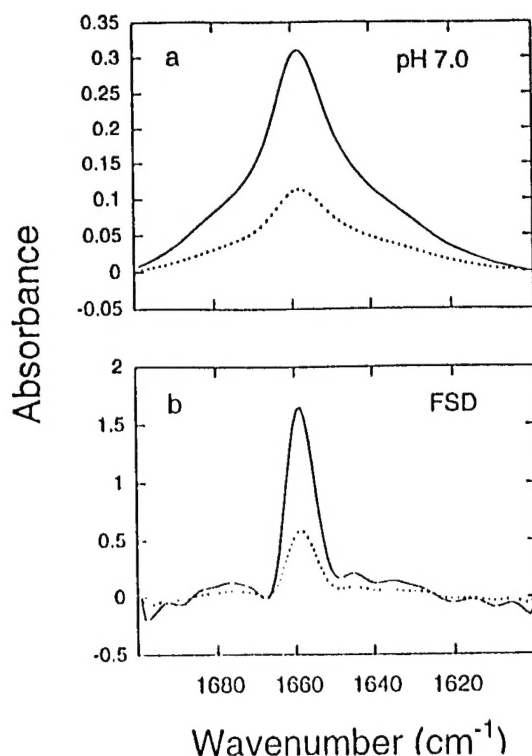


Figure 1: Polarized ATR FTIR spectra of the amide I band of neuTM (a) along with its Fourier self-deconvolution (b). Spectra were obtained of neuTM incorporated into DMPC multilayers at pH 7.0 using parallel (solid lines) and perpendicularly (dashed lines) polarized light.

Polarized IR spectra of the neu*TM incorporated into DMPC bilayers at pH 7.0 are quite different from those of neuTM. Figure 2 (left) presents the Fourier self deconvolutions of polarized ATR-FTIR spectra of neu*TM incorporated into DMPC bilayers. The spectra were obtained with parallel (solid lines) and perpendicular (dashed lines) polarized light as described in [16]. The amide I band is centered at 1655 cm⁻¹, characteristic of helical secondary structure. Increasing the pH from pH 5.5 to pH 7.0 results in a substantial increase in a band at 1630 cm⁻¹ that may be attributed to extended β -structure. The orientation of the helical region of the peptide is estimated from the dichroic ratio ($A_{\text{parallel}}/A_{\text{perpendicular}}$) of the amide I band at 1655 cm⁻¹. The measured dichroic ratio at pH 5.5 corresponds to a helix angle of 25° relative to the bilayer normal. The orientation is roughly the same at pH 8.5.

The most straightforward interpretation of the FTIR data is that increasing the pH results in local unfolding of the peptide. The current hypothesis is that protonation of Glu 664 allows the peptide to fold into a long α -helix spanning the membrane stretching from the C-terminus through position 664. Deprotonation is thought to lead to unfolding of the helix from Glu 664 to the N-terminus of the protein. This suggests that Glu 664 titrates with a pKa between 5.5 and 7. This is a substantial increase over the 4 - 4.5 solution pKa of glutamic acid. However, an increased pKa might be expected to result from the surface charge on DMPC bilayers. Previous studies on membrane lipids and fatty acids have shown that the apparent pKa increases near the membrane surface [28-30]. The apparent pKa corresponds to the bulk pH at which half of the COOH groups are protonated, and should be distinguished from the intrinsic pKa which corresponds to the surface pH at which half of the COOH groups are protonated.

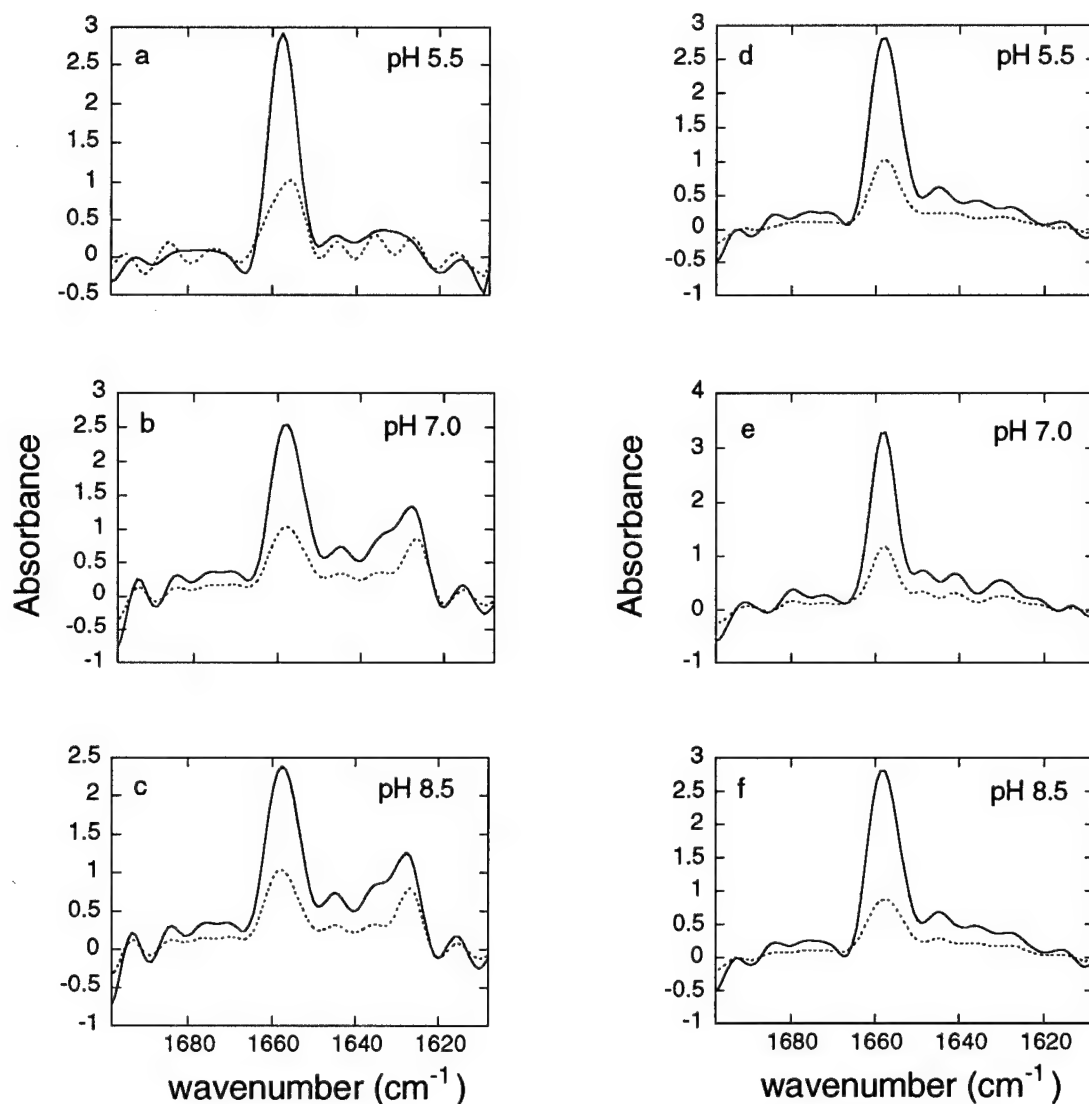


Figure 2: (Left) Polarized FTIR spectra of the amide I band of neu*TM in DMPC multilayers. Fourier self deconvolutions are shown of spectra obtained of oriented membranes at pH 5.5 (a) pH 7.0 (b) and pH 8.5 (c). Spectra were obtained with parallel (solid) and perpendicularly (dashed) polarized light.

(Right) Polarized FTIR spectra of the amide I band of neu*TM in DMPC:DMPS multilayers. Fourier self deconvolutions are shown of spectra obtained of oriented membranes at pH 5.5 (d) pH 7.0 (e) and pH 8.5 (f). Spectra were obtained with parallel (solid) and perpendicularly (dashed) polarized light.

In order to establish how membrane surface charge influences the pKa of the Glu 664, we incorporated 14% DMPS into the DMPC vesicles. DMPS is the major negatively charged lipid in mammalian cell membranes and usually ranges in concentration from 10 - 20%. The FSDs of the amide I band of neu*TM in DMPC:DMPS membranes are shown in Figure 2 (d-f). The frequency and intensity of the FSD band at 1655 cm^{-1} argue that the peptide is predominantly helical. The orientation is significantly more transmembrane than in DMPC vesicles.

Finally, CD spectra of neuTM and neu*TM in DMPC were obtained to compare with the results from IR. Both methods can address the global secondary structure of the peptides. The results from CD are more difficult to quantitate due to problems associated with light-scattering. The advantage of CD, however, is that spectra are obtained of vesicles in dilute solution rather than of multilayers that have been oriented as a dried film on a Ge crystal.

In Figure 3a, the spectrum of neuTM (grey line) exhibits a larger helical signal than neu*TM (black line) at pH 7. This is consistent with the interpretation from the IR data that the N-terminus of neu*TM unfolds above the pKa of Glu 664. An attempt was made to titrate the CD signal in a manner analogous to the IR titration. The spectra in Figure 3b were obtained at pH 5, 6 and 7 and show a slight loss of helical signal as the pH is raised, again consistent with the IR data.

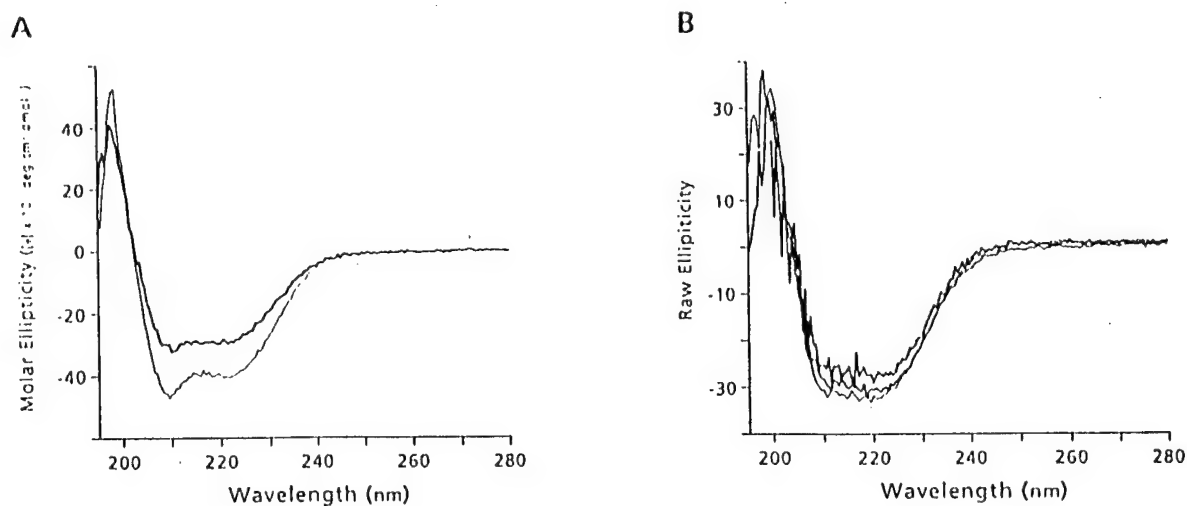


Figure 3: CD spectra of neuTM and neu*TM. (a) CD spectra of neuTM (grey line) and neu*TM (black line) at pH 7. (b) CD spectra of neu*TM as a function of pH. There is slightly less helical signal as the pH is changed from pH 5 to pH 6 and pH 7.

Task 1b: Rotational Resonance NMR Studies of the Local Secondary Structure of neuTM and neu*TM.

The predominant secondary structural motif in transmembrane domains is the α -helix. β -strands have also been found, most notably in the porins, which form a "barrel" of 16 β -strands in the outer membrane of gram negative bacteria. In addition, some membrane proteins appear to have combinations of α -helix and β -strand. The nicotinic acetylcholine receptor, for example, is thought to consist of a central ion pore made of five transmembrane helices surrounded by membrane-spanning β -sheet.

Although current MAS NMR methods are unable to generate the matrix of distance constraints needed to position every residue in a membrane protein, selected internuclear distance measurements can identify local α -helix or β -strand structure. These distances are short range ($< 6-7$ Å) and occur between residues close together in the amino acid sequence. In an α -helix with 3.6 residues per turn, the amino acid sequence spirals back on itself within four residues. Consequently, α -helix structure is readily identified by measurements between residue n and residue $n+3$ or $n+4$.

Rotational resonance NMR spectra of neuTM and neu*TM were obtained to establish the local secondary structure in the region of position 664. Specifically, distances were measured between the methyl group of Ala 668 and the backbone carbonyl of Gly 665, and between the α -carbon of Gly 665 and the backbone carbonyl of Thr 662. These positions are separated by 4.5 Å and 4.8 Å, respectively, in canonical α -helices.

The $n=1$ magnetization exchange curves of the four peptides studied are presented in Figures 4a and b along with simulations for $\text{CH}_2 \leftrightarrow \text{C=O}$ and $\text{CH}_3 \leftrightarrow \text{C=O}$ spin pairs at different internuclear distances. The experimental intramolecular magnetization exchange curves were generated by integration of the $^{13}\text{CH}_2$ and $^{13}\text{C=O}$ or $^{13}\text{CH}_3$ and $^{13}\text{C=O}$ peaks in the RR NMR spectra. Due to the strong proton couplings in the $^{13}\text{CH}_2$ group, the influence of high speed MAS on CP efficiency is minimal. This is not the case for the $^{13}\text{C=O}$ group that has no directly bonded protons and exhibits large oscillations in its Hartmann-Hahn matching profile at high MAS [32]. One of the advantages of the VACP sequence used in these experiments is that Hartmann-Hahn profile for $^{13}\text{C=O}$ resonance is broadened to resemble that of the $^{13}\text{CH}_2$ group. This results in more stable intensities over the course of the RR NMR experiment. A comparison of the simulated curves and the scatter in the experimental data points shows that the precision in these measurements is about 0.2 Å.

The natural abundance intensity contributing to each resonance was determined by integration of a spectrum obtained of the reconstituted unlabeled neuTM peptide. Since we typically observe an oscillation in the intensity of the time points below ~ 1 msec, possibly due to probe ringdown, the intensities of the first three time points (100 μsec , 500 μsec and 1 msec) have been averaged and normalized to a value of 1.0. Simulations of the magnetization exchange curves were performed using the methods of Levitt et al. [12]. Several parameters must be defined for these calculations. The chemical shift tensors for the C=O and CH_2 groups are taken from studies on alanylalanine and glycine. The relative shift tensor orientations cannot be defined without assuming a secondary structure. However, this is not a problem for the $n=1$ exchange curves which are not sensitive to the tensor orientations [12]. The two parameters that dominate the calculated exchange rates are the dipolar coupling, which is related to the internuclear distance, and the zero quantum T_2 relaxation.

The value of the dipolar coupling was varied in the simulations to correspond to distances between 4.0 and 5.5 Å. The zero quantum T_2 was taken from crystalline model compounds.

The similarity of the curves for the Ala 668 to Gly 665, and the Gly 665 to Thr 662 distances clearly shows that there is no change in local secondary structure in the region of position 664 in going from neuTM to neu*TM. These data rule out the model for receptor activation proposed Brandt-Rauf et al. [5] who suggested that change in the secondary structure occurs between the transmembrane domains of neuTM and neu*TM in the region of position 664.

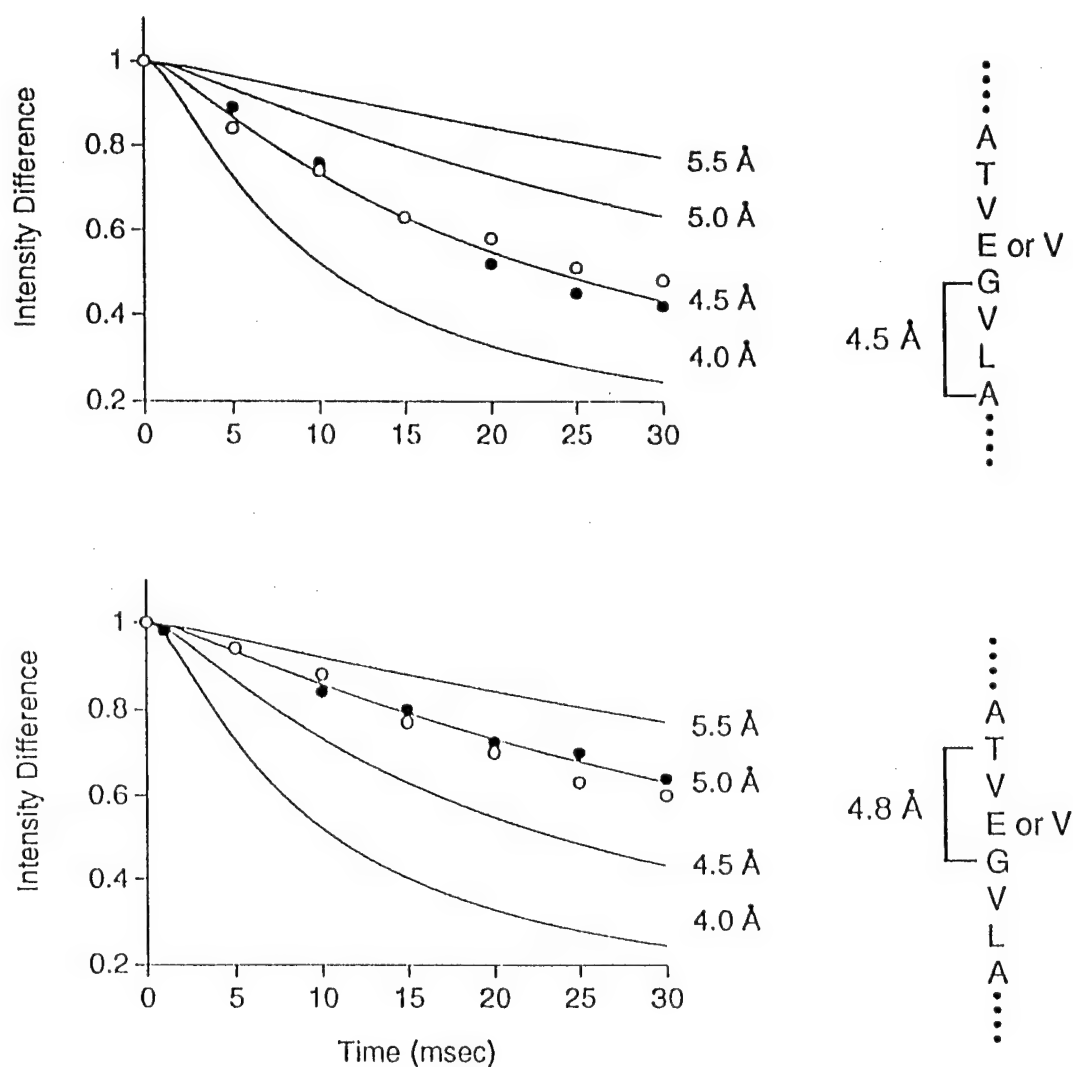


Figure 4: Rotational resonance NMR magnetization exchange curves of neuTM and neu*TM along with simulations. The neuTM and neu*TM peptides were reconstituted into DMPC bilayers at pH 7 and pH 5.5, respectively.

Task 2a: Magic Angle Spinning NMR Studies of the Protonation State and pKa of Glu 664 in neu*TM.

The FTIR data described above (Task 1a) argued that the N-terminal region of neu*TM unravels when the Glu 664 side chain carboxyl group is charged. In order to determine whether the Glu 664 side chain titrates with a pKa between 5.5 and 7.0, MAS NMR spectra were obtained of neu*TM labeled with [5- ^{13}C] glutamate reconstituted into DMPC bilayers. The ^{13}C chemical shift of the Glu 664 carboxyl group is sensitive to its protonation state with the isotropic chemical shift moving downfield upon deprotonation [27].

Figure 5 presents MAS NMR spectra of the neu*TM domain in DMPC bilayers at pH 5.5 (a), pH 7.0 (b) and pH 8.5 (c). In Figure 5a, the resonance at 179.6 ppm is assigned to the side chain carboxyl of Glu 664 based on a comparison with unlabeled peptide. Increasing the pH to 7.0 (Figure 4b) results in the appearance of a second resonance at 180.9 ppm. The intensity of the 180.9 ppm resonance increases in intensity when the pH is further increased to 8.5 (Figure 5c). Integration of the intensities of a full pH series from pH 5.5 to 8.5 indicates that the apparent pKa of Glu 664 in DMPC bilayers is ~6.5. Again, this is a substantial increase over the 4 - 4.5 solution pKa of glutamic acid.

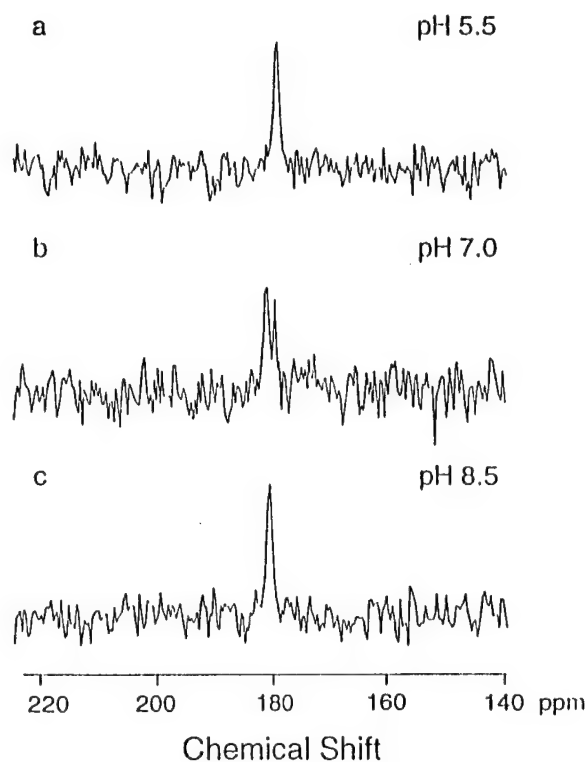


Figure 5: MAS NMR spectra of neu*TM at pH 5.5 (a), 7.0 (b) and 8.5 (c) in DMPC multilayers. Spectra were obtained at a ^{13}C frequency of 90.4 MHz with a MAS speed of 5.000 kHz. The spectra shown are actually difference spectra where a spectrum of unlabeled neu reconstituted in DMPC has been subtracted. The temperature was maintained at -20°C . At higher temperatures, the two resonances broaden and collapse into a single line due to exchange.

Integration of the intensities of a pH series from pH 5.5 to 8.5 indicates that the apparent pK_a of Glu 664 in DMPC bilayers is ~6.5 (Figure 6). This represents a substantial shift (~2 pH units) from the intrinsic pK_a of glutamate. A pK_a of 6.5 indicates that the Glu 664 side chain is still charged at physiological pH and unable to partition into the membrane. A further increase in the pK_a, however, is observed for neu*TM in DMPC:DMPS membranes which bear a net negative surface charge. The MAS NMR measurements of 5-[¹³C]-Glu 664 neu*TM in DMPC:DMPS membranes correlate with the FTIR results and show that the pK_a shifts to ~9. The large shift in the pK_a of the Glu 664 carboxyl group relative to the carboxyl group in the phosphatidylserine headgroup in DMPS may reflect stabilization of the protonated Glu 664 side chain due to dimerization.

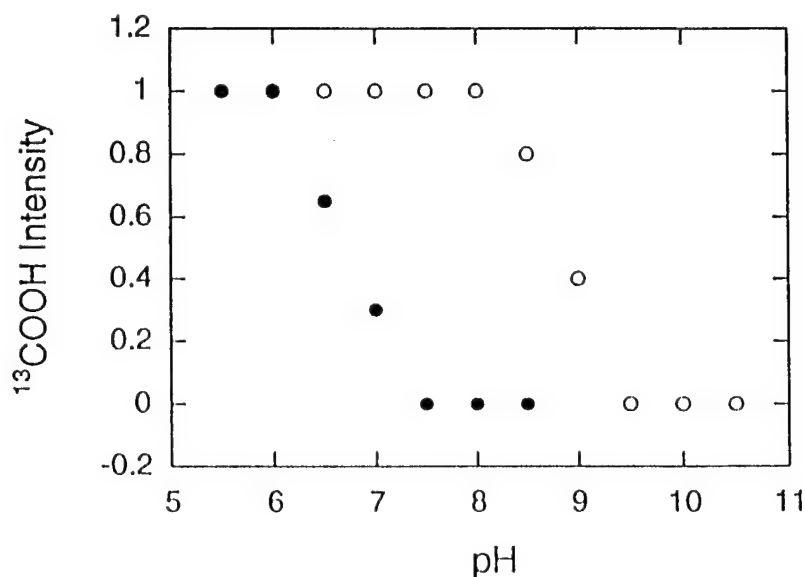


Figure 6: Integrated intensity of the 5-[¹³C]-Glu 664 resonance in the neu*TM sequence as a function of pH. Titration curves are shown for the neu*TM peptide reconstituted into DMPC (●) and into DMPC:DMPS (○) multilayers.

The strength of hydrogen bonds formed by the Glu 664 δ-carboxyl group can be determined from the principal elements of the ¹³C chemical shift tensor. The principal tensor elements (σ_{11} , σ_{22} and σ_{33}) can be calculated from the integrated intensities of the rotational side bands observed in a MAS NMR spectrum obtained at low spinning speed [35]. Based on an extensive series of model compounds, McDermott and coworkers found a strong correlation between the σ_{22} element of the chemical shift tensor and the O···H hydrogen bonding distance between the carbonyl of a protonated acid and its nearest proton donor [36]. Strong hydrogen bonding interactions between two carboxyl groups correlated with σ_{22} values greater than ~170 ppm, while weak hydrogen bonding interactions between a carboxyl group and a carbonyl or amide group correlated with σ_{22} values less than ~170 ppm. In contrast, the σ_{11} and σ_{33} elements are largely insensitive to hydrogen bonding interactions.

In order to provide a comparison with the neu*TM sequence, we first obtained a series of MAS NMR spectra of crystalline L-glutamic acid. The carboxyl groups in the crystal structure are strongly hydrogen bonded [37]. Figure 7a presents the MAS NMR spectrum of double ¹³C-labeled glutamic acid using a MAS frequency of 2.5 kHz. The isotropic resonance of the side chain δ-

carboxyl is observed at 178 ppm and is flanked by rotational side bands spaced by the MAS frequency. The +1 and -1 side bands have roughly the same intensity. The σ_{22} tensor element derived from an analysis of side band intensities is at 174 ppm; this is the largest downfield σ_{22} shift observed for protonated carboxyl groups in an extensive series of model compounds [36]. The backbone carboxyl resonance is at 176 ppm. The +1 side band is more intense than both the centerband and -1 side band and reflects an upfield shift of the σ_{22} element to 165 ppm. Smaller shifts are observed for the σ_{11} and σ_{33} elements.

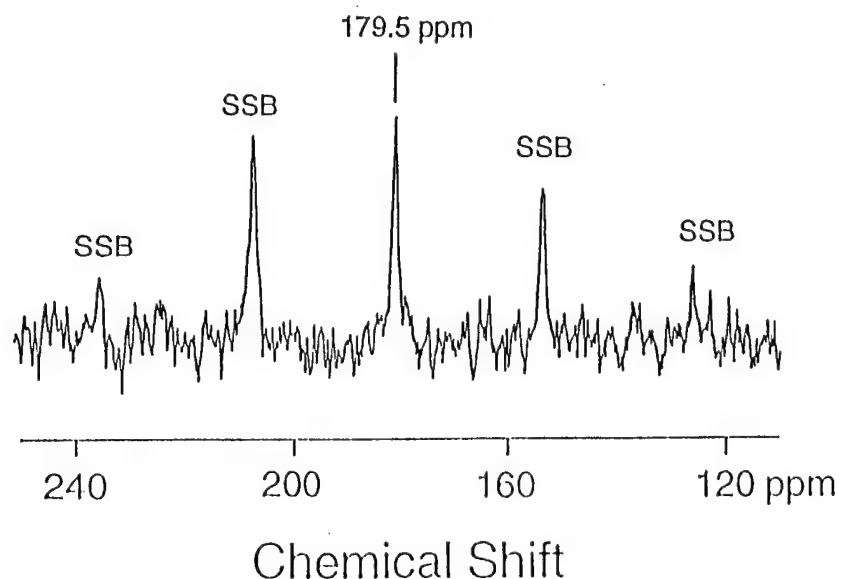


Figure 7: MAS spectra of crystalline 1,5- ^{13}C glutamic acid (a) and the neu* peptide in DMPC:DMPS membranes at pH 6.0 (b). The MAS frequency was 2.5 kHz.

Figure 7b presents a difference MAS NMR spectrum between unlabeled neu* and 5- ^{13}C -E664 - labeled neu* obtained under the same conditions as above. The difference spectrum exhibits only the resonances resulting from the 5- ^{13}C -labeled carboxyl group. The -1 sideband appears to be slightly more intense than the +1 side band suggesting a downfield shift in the σ_{22} tensor element. Side band analysis confirms this observation. The σ_{22} element shifts from 174 ppm to 183 ppm indicating a *stronger* H-bonding interaction for the δ -carboxyl group compared to crystalline glutamic acid. Based on a linear correlation between σ_{22} and the O...H hydrogen bond distance [36], the 183 ppm shift would correspond with a 1.5 Å O...H separation.

Figure 8 presents a model that incorporates the results described above. First, the region C-terminal to position 664 is helical and oriented roughly perpendicular to the membrane plane. When the Glu 664 carboxyl group is deprotonated, the region N-terminal to position 664 unfolds and the COO- group is exposed to the polar membrane interface. Protonation allows the peptide to adopt a helical conformation oriented perpendicular to the membrane plane. The pKa of the Glu 664 side chain is shifted by the membrane surface charge. Under conditions approximating those in native membranes, the carboxyl group readily partitions into the membrane. The high pKa observed for the Glu 664 carboxyl group and increased orientation in DMPC:DMPS membranes may reflect dimerization of the peptides in membranes.

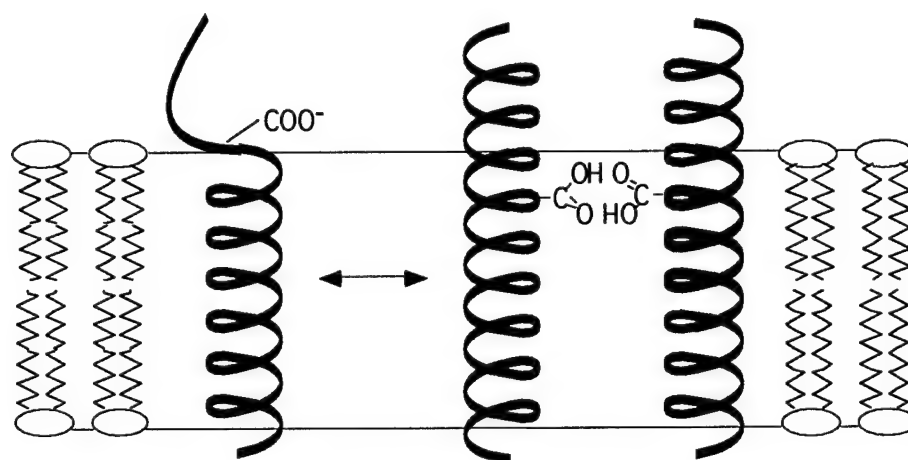


Figure 8: Model illustrating the influence of membrane surface potential on the pKa of Glu 664 in neu*TM.

Task 2b: Amide Exchange Measurements on neuTM and neu*TM.

Position 664 is the only established contact point in the neu* dimer. The major thrust of this section of the proposal was to map out the interacting surfaces in the transmembrane dimer and determine whether or not there are multiple contact points. The original approach was to use amide exchange of the backbone NH groups in the transmembrane region of the neuTM and neu*TM. This approach failed for reasons described below. However, a new approach has been developed and shown to be capable of establishing the rotational orientation of helices in membrane bilayers. The approach involves the novel use of cysteine sulfhydryl exchange. In this section, I will first outline why the amide exchange experiments failed and then first discuss the cysteine sulfhydryl exchange methodology and the specific experiments to determine if there are contact sites other than near position 664.

Amide exchange methods have long been used to assign exposed residues in small soluble proteins (< 30kD). The proposal was to adapt amide exchange measurements in a fashion described by Dempsey using solution NMR methods [38]. As a first order experiment to test whether this approach would work, we measured the exchange rates of amide groups near position 664 using FTIR spectroscopy. This was relatively straightforward since we had a number of isotopically labeled peptides and were making IR measurements to determine the global secondary structure and orientation of neuTM and neu*TM. Isotopic labels are able to shift a specific amide I vibration away from the broad amide I envelope [39] so that the accessibility of a single backbone site to deuterium exchange can be determined. We found that exchange takes place exceedingly slowly within the transmembrane region of neuTM and neu*TM α -helices in bilayers, and consequently did not pursue these studies further.

However, while this conclusion was being reached, we were working on a method for determining the lipid-exposed surfaces of membrane proteins using cysteine sulfhydryl exchange [31].

Single cysteines provide unique markers for exchange and do exchange with D₂O. The SH vibrational mode is located at 2540 - 2590 cm⁻¹ away from other protein vibrations and shifts roughly -700 cm⁻¹ upon deuteration. The SH group is more acidic and more mobile than the backbone NH, and consequently exhibits faster exchange rates in membrane environments. The SH groups in helix interfaces are protected from exchange in a manner analogous to the NH groups buried in the interior of soluble proteins. However, we have shown that the SH groups in the lipid interface undergo rapid SH to SD exchange from water which is known to readily permeate the lipid membrane.

We have only recently begun to carry out SH exchange experiments on neuTM and neu*TM. The first set of cysteine sulfhydryl exchange studies target the helical turns N-terminal to position 664. Cysteines have been incorporated into residues 656, 657, 658 and 660 in peptides with either valine or glutamate at position 664.

AEQRASP-C-TFIIATV-x-GVLLFLILVVVVGILIKRRRYK x = E OR V

AEQRASPV-C-FIIATV-x-GVLLFLILVVVVGILIKRRRYK

AEQRASPVT-C-IIATV-x-GVLLFLILVVVVGILIKRRRYK

AEQRASPVTFII-C-TV-x-GVLLFLILVVVVGILIKRRRYK

The sequences for the first four peptides being targeted are given above. If one of the sites between 656-660 is protected, then longer peptides will be synthesized with cysteine substitutions at positions 3-5 residues N-terminal to the protected sites. All experiments will be carried out under reducing conditions. Observation of an SH band at 2560 cm⁻¹ insures that samples are reduced.

The results will also be correlated with cysteine cross-linking experiments being undertaken by Prof. David Stern (Department of Pathology, Yale University) on the full length receptor who is assessing the ability of site specific cross-links in the transmembrane and juxtamembrane domains to activate the receptor (unpublished results).

We are confident that this approach on the neu receptor transmembrane domain based on our studies with the transmembrane domains of phospholamban and glycophorin A [31].

Task 3a: Rotational Resonance NMR Measurements of Interhelical Contacts in neu*TM.

One of the goals of the proposed research was to test various models for the structure of neu*TM and the structural changes occurring between neuTM and neu*TM. The first model mentioned in the introduction involved a change in the secondary structure of the transmembrane domain between neuTM and neu*TM. Brandt-Rauf et al. [5] calculated that the minimum-energy conformation of neuTM contains a sharp bend at positions 664 and 665, neu*TM exists as an α -helix. The intrahelical rotational resonance measurements discussed under Task 1b have ruled out such a change in secondary structure.

Two additional models for receptor activation involved dimerization via hydrogen-bonding interactions [6]. In the first model, the helices are thought to be held in the "active" state by hydrogen bonding between the Glu 664 COOH side chain on one helix and the Glu 664 COOH side chain on the opposing helix. In the second model, the hydrogen bonding interactions are postulated to be between the Glu 664 side chain and the peptide backbone carbonyl group of Ala 661 of the second helix. These two models can be distinguished by selected $^{13}\text{C}\dots^{13}\text{C}$ and $^{13}\text{C}\dots^{15}\text{N}$ distance measurements. Below several distances are compared that might be used to distinguish the two models. These distances were derived from molecular modeling studies.

	-COOH...HOOC- Model	-COOH...O=C- Model
$ \begin{array}{c} \text{O} \quad \text{HO} \\ \parallel \quad \parallel \\ 664 - {}^{13}\text{C} \quad {}^{13}\text{C} - 664 \\ \backslash \quad / \\ \text{OH} \quad \text{O} \end{array} $	3.4 Å	3.4 Å
$ \begin{array}{c} \text{O} \quad \\ \parallel \quad \text{H}_2{}^{13}\text{C} - 665 \\ \backslash \quad / \\ \text{OH} \quad \text{O} \end{array} $	5.0 Å	3.8 Å
$ \begin{array}{c} \text{O} \quad \\ \parallel \quad \text{H}_2{}^{13}\text{C} - 665 \\ \backslash \quad / \\ {}^{15}\text{NH}_2 \quad \text{O} \end{array} $	6.8 Å	4.1 Å
$ \begin{array}{c} \text{O} \quad \\ \parallel \quad \text{H}_2{}^{13}\text{C} - 661 \\ \backslash \quad / \\ {}^{15}\text{NH}_2 \quad \text{O} \end{array} $	5.6 Å	4.8 Å

Figure 9 presents the results of a rotational resonance magnetization exchange experiment that targets the distance between the Glu 664 ($^{13}\text{COOH}$) and Gly 665 ($^{13}\text{CH}_2$) residues across the helix interface. Neu*TM peptides containing a single ^{13}C label were combined in a 5:1 ($^{13}\text{CH}_2$: $^{13}\text{COOH}$) molar ratio using a peptide:lipid ratio of 1:30. The non-stoichiometric combination of peptides insures that >90% of the $^{13}\text{COOH}$ -labeled peptides are paired with a $^{13}\text{CH}_2$ -labeled peptide in a dimer complex. In Figure 9, only the intensity of the $^{13}\text{COOH}$ label is plotted as a function of the magnetization mixing time. This experimental approach is similar to that used to characterize the packing of residues in the interface of the glycoporphin A transmembrane dimer [11]. The distance

between the two ^{13}C labels based on simulations [12] is $\sim 5.0 \text{ \AA}$ consistent with the $-\text{COOH}\dots\text{HOOC}-$ model.

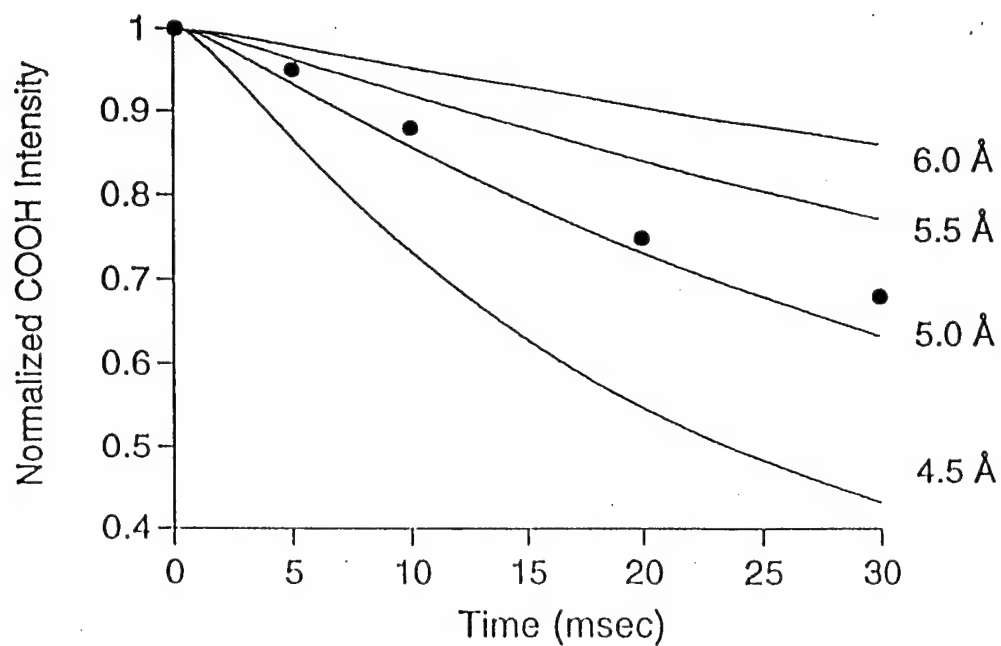


Figure 9: Interhelical rotational resonance NMR measurements of neu*TM. The $\sim 5.0 \text{ \AA}$ distance measured between Glu 664 (COOH) and Gly 665 (CH₂) across the helix interface is consistent with the $-\text{COOH}\dots\text{HOOC}-$ model.

Task 3b. Rotational Echo Double Resonance (REDOR) NMR Measurements of Interhelical Contacts in neu*TM.

The rotational resonance measurements of a specific $^{13}\text{C}\dots^{13}\text{C}$ distance across the dimer interface in the neu receptor provides the first evidence for the packing arrangement in the vicinity of residue 664. An additional distance constraint that can serve to distinguish the two models for interhelical hydrogen-bonding is between the side chain amine nitrogen of glutamine 664 and the backbone carbonyl carbon of alanine 661. As mentioned above, glutamine at position 664 is equally as transforming as glutamate since it can form the same hydrogen-bonds, however, facilitates the NMR measurements by providing an ^{15}N group in the area of interest that can be used for REDOR experiments. The REDOR experiment requires collecting a ^{13}C spectrum with and without dephasing pulses on the ^{15}N channel. The intensity differences between the two spectra can be related to the $^{13}\text{C}\dots^{15}\text{N}$ dipolar coupling, which can in turn be related to the internuclear distance. This has been done for the Gln 664 (^{15}N) - Ala 661 ($1\text{-}^{13}\text{C}$) experiment in which peptides containing single isotopic labels were reconstituted in a ratio of 5:1 ($^{15}\text{N}:^{13}\text{C}$) in a manner similar to that of the rotational resonance experiments. The pulse sequence used for the experiment has been described by Schaefer and Gullion [19,20]. The REDOR intensity changes for this spin pair are presented in Figure 10.

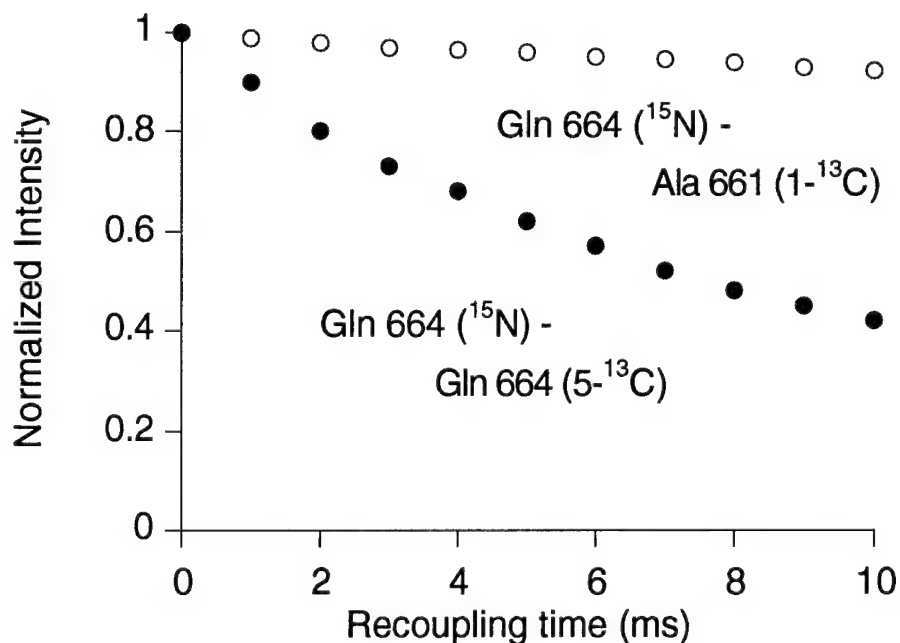


Figure 10: REDOR exchange plot for neu*TM. The two curves are for the spin pairs indicated.

We are now in the process of analyzing this data. However, the preliminary analysis yields a distance of $>5.5 \text{ \AA}$ using the relationship,

$$\Delta S/S = K D^2 N_c^2 \omega_r^{-2}$$

where ΔS is the REDOR difference spectrum, S is the original REDOR spectrum without dephasing pulses, K is a dimensionless constant equal to 1.066, D is the dipolar coupling, N_c is the number of rotor cycles (32-64 in our experiments) and ω_r is the MAS frequency (~ 4 kHz).

As a control for these experiments, we also measured the interhelical distance between the ^{15}N side chain position of Gln 664 and the $^{13}\text{C}=\text{O}$ of the amide functional group of Gln 664 on a second peptide. This distance is predicted to be close ($\sim 3.5 - 4.0$ Å) in both of the models for Gln/Glu 664 hydrogen bonding. The REDOR curve in Figure 10 is consistent with a short (< 4.5 Å) distance. Together, the REDOR distances (although still in a preliminary stage of analysis) are consistent with side chain - side chain hydrogen bonding interactions, rather than side chain - backbone interactions, as the driving force for receptor dimerization in neu*TM.

Task 3c. Molecular Dynamics and Energy Minimization of neu*TM.

Our current efforts in molecular modeling have generated the structure of the neu* transmembrane helix shown in Figure 11. The emphasis for the modeling studies has been to obtain structures that can be experimentally tested and refined. The polarized IR and MAS NMR measurements described above provide the structural constraints. The modeling efforts were undertaken in parallel with the experimental work. The two programs used for molecular modeling were Discover and XPLOR. Both programs have energy minimization and molecular dynamics routine. The only conclusion that can be drawn from these studies to date is that it is possible to obtain a low energy structure of neu*TM helices that interact via the Glu 664 COOH groups. The structure shown has a left handed coiled coil geometry with a helix crossing angle of $\sim 20^\circ$. It has not been possible to model a well packed dimer having $-\text{COOH} \cdots \text{HOOC}-$ interactions and a right-handed coiled coil geometry. One additional point about the structure shown is that the Glu 664 side chain is relatively well-packed against Gly 665. This is consistent with the mutagenesis studies of Stern and coworkers who have shown that a glycine at this position is critical for receptor activation by the Glu 664 mutation [4].

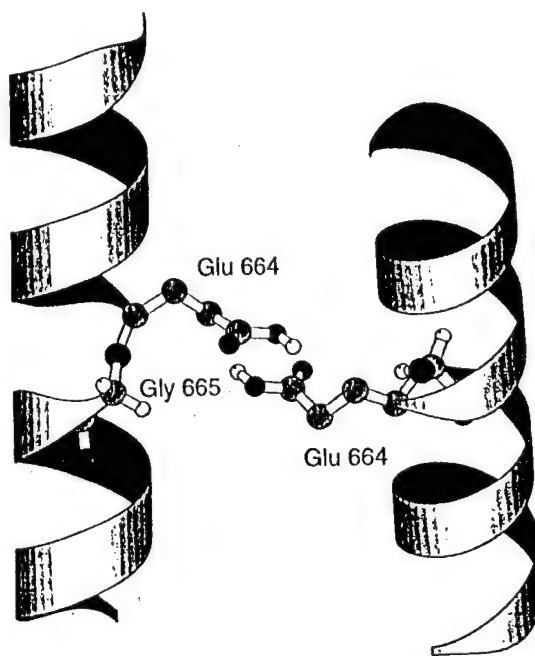


Figure 11: Molecular model of neu*TM.

CONCLUSIONS

The objective of this Exploratory Award was to establish whether MAS NMR and polarized IR methods could be applied to obtain high resolution structural constraints on the transmembrane domain of the neu/erbB-2 receptor in membrane environments. Such data would be able to address specific models for receptor activation by the transforming Glu 665 mutation. The ultimate goal has been to obtain high resolution 3D structures of the neuTM and neu*TM domains that can be used to establish the activation mechanism and possibly serve as guides to the design of competitive inhibitors. The results presented above demonstrate that the approach outlined was largely successful and have provided the ground work for further studies. The conclusions that can be drawn thus far are as follows:

- The neuTM and neu*TM peptides form extended helical structures oriented perpendicular to the membrane surface.
- The high pKa of the COOH group in neu*TM reconstituted into DMPC:DMPS membranes indicates that the Glu 664 carboxyl group is buried in the membrane interior, possibly in the dimer interface between TM domains.
- The COOH chemical shift tensor of Glu 664 correlates with extremely strong hydrogen bonding.
- The intrahelical rotational resonance measurements indicate that there is no change in local secondary structure in the vicinity of position 664 due to the valine to glutamic acid substitution.
- The interhelical rotational resonance and REDOR measurements are consistent with the -COOH...HOOC- model for helix interactions.

REFERENCES

- 1 Bargmann CI, Weinberg RA. Oncogenic activation of the neu-encoded receptor protein by point mutation and deletion. *EMBO J* 1988; 7:2043-2052.
- 2 Bargmann CI, Hung M-C, Weinberg RA. Multiple independent activations of the neu oncogene by a point mutation altering the transmembrane domain of p185. *Cell* 1986; 45:649-657.
- 3 Bargmann CI, Hung M-C, Weinberg RA. The neu oncogene encodes an epidermal growth factor receptor-related protein. *Nature* 1986; 319:226-230.
- 4 Cao H, Bangalore L, Bormann B-J, Stern DF. A subdomain in the transmembrane domain is necessary for p185neu* activation. *EMBO J* 1992; 11:923-932.
- 5 Brandt-Rauf PW, Rackovsky S, Pincus MR. Correlation of the structure of the transmembrane domain of the neu oncogene-encoded p185 protein with its function. *Proc Natl Acad Sci U S A* 1990; 87:8660-8664.
- 6 Sternberg MJ, Gullick WJ. Neu receptor dimerization. *Nature* 1989; 339:587.
- 7 Weiner DB, Liu J, Cohen FA, Williams WV, Greene MI. *Nature* 1989; 339:230-231.
- 8 Lofts FJ, Hurst HC, Sternberg MJE, Gullick WJ. Specific short transmembrane sequences can inhibit transformation by the mutant neu growth factor receptor in vitro and in vivo. *Oncogene* 1993; 8:2813-2820.
- 9 Arkin IT, Rothman M, Ludlam CFC, Aimoto S, Engelman DE, Rothschild K, Smith SO. Structural model of the phospholamban ion channel complex in phospholipid membranes. *J Mol Biol* 1995; 248:824-834.
- 10 Smith SO, Jonas R, Braiman M, Bormann BJ. Structure and orientation of the transmembrane domain of glycophorin A in lipid bilayers. *Biochemistry* 1994; 33:6334-6341.
- 11 Smith SO, Bormann BJ. Determination of helix-helix interactions in membranes by rotational resonance NMR. *Proc Natl Acad Sci USA* 1995; 92:488-491.
- 12 Levitt MH, Raleigh DP, Creuzet F, Griffin RG. Theory and simulations of homonuclear spin pair systems in rotating solids. *J Chem Phys* 1990; 92:6347.
- 13 Gullion T, Schaefer J. Detection of weak heteronuclear dipolar coupling by rotational echo double-resonance nuclear magnetic resonance. *Adv Magn Reson* 1989; 13:57-83.
- 14 Hing AW, Vega S, Schaefer J. Transferred-echo double resonance NMR. *J Magn Reson* 1992; 96:205-209.
- 15 Tycko R, Smith SO. Symmetry principles in the design of pulse sequences for structural measurements in magic angle spinning nuclear magnetic resonance. *J Chem Phys* 1993; 98:932-943.

- 16 Colombo MG, Meier BH, Ernst RR. Rotor-driven spin diffusion in natural-abundance ^{13}C Spin Systems. *Chem Phys Lett* 1988; 146:189-196.
- 17 Peersen OB, Yoshimura S, Hojo H, Aimoto S, Smith SO. Short range distance determination in integral membrane proteins by magic angle spinning NMR. *J Am Chem Soc* 1992; 114:4332-4335.
- 18 Peersen OB, Smith SO. Rotational resonance NMR of biological membranes. *Concepts in Magn Reson* 1993; 5:305-317.
- 19 Bork V, Gullion T, Hing A, Schaefer J. Measurement of ^{13}C - ^{15}N coupling by dipolar-rotational spin-echo NMR. *J Magn Reson* 1990; 88:523-532.
- 20 Gullion T, Schaefer J. Rotational-Echo Double-Resonance NMR. *J Magn Reson* 1988; 81:196-200.
- 21 Braiman MS, Rothschild KJ. Fourier transform infrared techniques for probing membrane protein structure. *Ann Rev Biophys Biophys Chem* 1989; 17:541-570.
- 22 Kauppinen JK, Moffatt DJ, Mantsch HH, Cameron DG. Fourier self-deconvolution: A method for resolving intrinsically overlapped bands. *Appl Spectrosc* 1981; 35:271-276.
- 23 Byler MD, Susi H. Examination of the secondary structure of proteins by Deconvolved FTIR spectra. *Biopolymers* 1986; 25:469-487.
- 24 Bradbury EM, Brown L, Downie AR, Elliott A, Fraser RDB, Hanby WE. The structure of the ω -form of poly- β -benzyl-L-aspartate. *J Mol Biol* 1962; 5:230-247.
- 25 Miyazawa T, Blout ER. The infrared spectra of polypeptides in various conformations: amide I and amide II bands. *J Am Chem Soc* 1961; 83:712-719.
- 26 Tsuboi M. Infrared dichroism and molecular conformation of α -form poly- γ -benzyl-L-glutamate. *J Polymer Sci* 1994; 59:139-153.
- 27 Gu Z, Zambrano R, McDermott A. Hydrogen bonding of carboxyl groups in solid-state amino acids and peptides: comparison of carbon chemical shielding, infrared frequencies, and structures. *J Am Chem Soc* 1994; 116:6368-6372.
- 28 Hamilton JA, Cistola DP. Transfer of oleic acid between albumin and phospholipid vesicles. *Proc Natl Acad Sci USA* 1986; 83:82-86.
- 29 Kantor HL, Prestegard JP. Fusion of phosphatidylcholine bilayer vesicles: role of free fatty acid. *Biochemistry* 1978; 17:3592-3597.
- 30 Ptak M, Egret-Charlier M, Sanson A, Bouloussa O. A NMR study of the ionization of fatty acids, fatty amines and N-acylamino acids incorporated in phosphatidylcholine vesicles. *Biochim Biophys Acta* 1980; 600:387-397.

- 31 Arkin, I.T., Mackenzie, K., Aimoto, S., Engelman, D. and S.O. Smith (1996) Mapping the lipid exposed surface of membrane proteins. *Nature Struct. Biol.* 3, 240-243.
- 32 Metz G, Howard K, van Liemt WBS, Prestegard J, Lugtenburg J. and S.O. Smith (1995) NMR studies of ubiquinone location in oriented model membranes: evidence for a single motionally-averaged population. *J. Am. Chem. Soc.* 117: 564-565.
33. Lofts FJ, Hurst HC, Sternberg MJE, Gullick WJ. Specific short transmembrane sequences can inhibit transformation by the mutant neu growth factor receptor in vitro and in vivo. *Oncogene* 1993; 8:2813-2820
34. Cao H, Bangalore L, Bormann B-J, Stern DF. A subdomain in the transmembrane domain is necessary for p185neu* activation. *EMBO J* 1992; 11:923-932.
- 35 Herzfeld J, Berger, AE. Side band intensities in NMR spectra of samples spinning at the magic angle. *J. Chem. Phys.* 73, 6021-6030 (1980).
- 36 Gu Z, Zambrano R, McDermott A. Hydrogen bonding of carboxyl groups in solid-state amino acids and peptides: comparison of carbon chemical shielding, infrared frequencies, and structures. *J. Am. Chem. Soc.* 116, 6368-6372 (1994).
- 37 Sequeira A, Rajagopal H, Chidambaram R. A neutron diffraction study of the structure of L-glutamic acid.HCL. *Acta Cryst B*28, 2514-2519 (1972).
- 38 Dempsey CE. (1988) pH dependence of hydrogen exchange from backbone peptide amides of mellitin in methanol. *Biochemistry* 27, 6893-6901.
- 39 Ludlam C, Arkin T, Liu XM, Rothman M, Rath P, Aimoto S, Smith SO, Engelman D, Rothschild, KJ (1996) Fourier transform infrared spectroscopy and site-directed isotope labeling as a probe of local secondary structure in the transmembrane domain of phospholamban. *Biophys. J.* 70, 1728-1736.

Bibliography of Publications

1. Smith, S.O., Smith, C.S. and B.J. Bormann (1996) Strong hydrogen bonding interactions involving a buried glutamic acid in the transmembrane domain of the neu/erbB-2 receptor. Nature Struct. Biol. 3, 252-258.
2. Groesbeek, M. and S.O. Smith (1996) Structure of the neu/erbB-2 transmembrane domain: implications for receptor activation. In preparation.

Abstracts:

1. Experimental NMR Conference, Asilomar, CA.
2. Tsukuba NMR Conference, Tsukuba, Japan
3. XVIth International Conference on Magnetic Resonance in Biological Systems

Personnel

Michel Groesbeek, Postdoctoral Research Associate

Steven Smith, Principal Investigator

Structural Studies of Signal Transduction by Membrane Proteins using Magic Angle Spinning NMR

May Han, Charles Smith, Thomas Sakmar and Steven O. Smith

Department of Molecular Biophysics and Biochemistry, Yale University, New Haven, CT 06520

Membrane proteins serve an array of functions in cell membranes ranging from receptors involved in signal transduction to ion channels. Our current research on signal transduction mechanisms mediated by protein conformational changes involves the visual pigment rhodopsin, the G-protein coupled receptor responsible for vision at low light intensities. NMR chemical shifts have been used to establish the major charge interactions in the retinal binding site of rhodopsin and bathorhodopsin (Han et al., Biochemistry 34, 1425). The NMR constraints are used to position 11-*cis* and distorted all-*trans* retinal chromophores in the interior of the apoprotein. Based on the protein-retinal interactions predicted by the structural model, mutagenesis studies have been undertaken to define the key contact sites. We find that G121 on helix 3 is crucial for maintaining an inactive pigment and that mutations at this position increase the ability of all-*trans* retinal to bind to and activate the protein. Furthermore, we show that second site mutations on helix 6 can 'rescue' the all-*trans* retinal activation caused by mutation of G121. These results provide direct evidence of structure-function complementation between helices in rhodopsin and provide the outlines of a mechanism for how the protein is activated by light.

Our research on the mechanisms of signal transduction mediated by receptor oligomerization has focused on the receptor tyrosine kinase encoded by the *neu/erbB-2* proto-oncogene. The *neu* receptor is constitutively activated by a single glutamic acid to valine substitution at position 664 in the predicted membrane-spanning domain. Measurements of the pKa and ^{13}C chemical shift anisotropy of Glu 664 reveal that the side chain carboxyl group is protonated and strongly hydrogen-bonded. These studies provide direct evidence for glutamate hydrogen-bonding interactions in the mechanism of receptor activation.

Abstract for the XVIth International Conference on Magnetic Resonance in Biological Systems
August 18-23, 1996, Keystone, Colorado

Structural Studies of Signal Transduction by Rhodopsin and the *neu* Receptor using Magic Angle Spinning NMR

Steven O. Smith, May Han, Charles Smith, Barbara J. Bormann and Saburo Aimoto

Department of Molecular Biophysics and Biochemistry, Yale University, New Haven, CT 06520 and Institute for Protein Research, Osaka, Japan

Membrane proteins serve an array of functions in cell membranes ranging from receptors involved in signal transduction to ion channels. The overall goal of our research is to understand the mechanisms of membrane proteins in chemical terms. Our current research on signal transduction mechanisms mediated by protein conformational changes involves the visual pigment rhodopsin, the G-protein coupled receptor responsible for vision at low light intensities. Absorption of light by the retinal chromophore of rhodopsin leads to a conformational change in the protein that allows binding of the G-protein transducin. Rhodopsin may serve as a model for the larger family of ligand-activated G-protein coupled receptors since the sequences and overall protein architecture are conserved. We have recently been able to position the retinal chromophore in the interior of the rhodopsin protein using NMR distance constraints. The NMR data constrain one of the carboxylate oxygens of Glu113 to be ~ 3 Å from the C₁₂ position of the retinal with the second oxygen oriented away from the conjugated retinal chain. Based on a structural model of rhodopsin developed from these studies in combination with biochemical and molecular biological approaches, we have been able to establish the key residues that are in contact with the retinal and responsible for protein activation.

Our research on the mechanism of signal transduction mediated by receptor oligomerization has focused on the transmembrane and juxtamembrane domains of several membrane proteins involved in signaling. In these systems, the 'signal' is often transduced by ligand-induced dimerization of receptor ectodomains leading to tyrosine kinase activation of the intracellular domains. The receptor tyrosine kinase encoded by the *neu/erbB-2* proto-oncogene is constitutively activated by a single glutamic acid to valine substitution at position 664 in the predicted membrane-spanning sequence of the receptor. Measurements of the pK_a and ¹³C chemical shift anisotropy of Glu 664 reveal that the side chain carboxyl group is protonated and strongly hydrogen-bonded. These studies provide direct evidence for glutamate hydrogen-bonding interactions in the mechanism of receptor dimerization and activation.

Abstract for the Tsukuba NMR Conference, Tsukuba, Japan May, 1996

STRONG HYDROGEN BONDING INTERACTIONS OF A BURIED GLUTAMIC ACID IN A MEMBRANE RECEPTOR PROTEIN

Charles Smith, Barbara Bormann and Steven O. Smith*
Department of Molecular Biophysics and Biochemistry,
Yale University, 266 Whitney Avenue, New Haven, CT 06520

The receptor tyrosine kinase encoded by the *neu/erbB-2* proto-oncogene is constitutively activated by a single glutamic acid to valine substitution at position 664 in the predicted membrane-spanning sequence of the receptor. We have explored the structural changes involved in receptor activation with polarized FTIR and magic angle spinning NMR spectroscopy. We show that the hydrophobic transmembrane sequence folds into a well-defined α -helical structure spanning the membrane bilayer. Measurements of the pKa and ^{13}C chemical shift anisotropy of Glu 664 reveal that the side chain carboxyl group is protonated and strongly hydrogen-bonded. These studies provide direct evidence for glutamate hydrogen-bonding interactions in the mechanism of receptor dimerization and activation.

Abstract for the Experimental Nuclear Magnetic Resonance Conference, Asilomar, Calif.
March, 1996

Strong hydrogen bonding interactions involving a buried glutamic acid in the transmembrane sequence of the neu/erbB-2 receptor

Steven O. Smith¹, Charles S. Smith¹ and Barbara J. Bormann²

The receptor tyrosine kinase encoded by the *neu/erbB-2* proto-oncogene is constitutively activated by a single valine to glutamic acid substitution at position 664 in the predicted membrane-spanning sequence of the receptor. We have explored the structural changes involved in receptor activation with polarized FTIR and magic angle spinning NMR spectroscopy. The hydrophobic transmembrane sequence folds into a well-defined α -helical structure spanning the membrane bilayer. Measurements of the pK_a and ^{13}C chemical shift anisotropy of Glu 664 reveal that the side chain carboxyl group is protonated and strongly hydrogen bonded. These studies provide direct evidence for glutamate hydrogen-bonding interactions in the mechanism of receptor dimerization and activation.

¹Department of Molecular Biophysics and Biochemistry, Yale University, 266 Whitney Avenue, Box 208114, New Haven, Connecticut 06520-8114, USA

²Boehringer-Ingelheim, Ridgefield, Connecticut 06877 USA

Correspondence should be addressed to S.O.S.

The *neu/erbB-2* proto-oncogene encodes a 185,000 M_r receptor tyrosine kinase that is involved in signal transduction across cell membranes^{1,2}. The receptor is part of the erbB family of receptor tyrosine kinases; it has two cysteine-rich extracellular domains, a single predicted helical membrane-spanning domain and an intracellular tyrosine kinase domain. Ligand-binding to the extracellular domain activates the kinase domain through receptor dimerization. The proto-oncogene may be transformed into an oncogene by a single point mutation of a valine residue to glutamic acid at position 664 within the hydrophobic transmembrane sequence³. This substitution is thought to stabilize receptor dimers and is the first instance of a mutation in the transmembrane domain of a growth factor receptor that leads to constitutive activation and cell transformation in the absence of ligand.

The position of the glutamic acid residue in the *neu* sequence is critical for receptor activation. Bargmann and Weinberg originally demonstrated that substitution of glutamic acid at positions 663 or 665 does not activate the receptor⁴. Stern and co-workers found that activation requires a three-residue motif, Val 663-Glu 664-Gly 665, whose position in the transmembrane sequence is tightly constrained^{2,5}. Furthermore, by moving this VEG sequence around in the transmembrane domain and by generating mutants that dimerize without activating the receptor, it was shown that dimerization alone is not sufficient to cause cell transformation^{2,5,6}. Together, these results argue that the transmembrane domain is not strictly passive in the signal transduction process and that specific interactions may be involved that determine the relative orientations of the predicted transmembrane helices. As a result, establishing the structure of the transmembrane

domain in the activated receptor (designated *neu**) is an important component in understanding the molecular mechanism of receptor signalling.

There are no direct experimental data on the structure of the *neu** transmembrane domain in membrane bilayers or for the points of contact in the receptor dimer. The structural questions raised by the seemingly simple V664E replacement are complicated by the low intrinsic pK_a of the glutamic acid side chain. In dimerization models for receptor activation, the Glu 664 side chain must be protonated and able to partition into the hydrophobic interior of the membrane. However, the glutamate carboxyl would be expected to be charged at neutral pH if it exhibits an intrinsic solution pK_a of 4.5–5. Two specific models have been proposed for how dimerization is linked to receptor activation. In both models, the Glu 664 carboxyl is predicted to be protonated. Based on sequence analyses of growth factor receptors, Sternberg and Gullick^{7,8} have suggested that a five residue sequence, Ala 661-X-X-Glu 664-Gly 665, is responsible for activation. In their model, specificity results from interhelical hydrogen bonds between the Glu 664 carboxylic acid side chain and the peptide backbone carbonyl group of Ala 661 in the second monomer. The small side chains of Ala 661 and Gly 665 are thought to be important for close helix packing. An alternative model based on conformational energy calculations argues that receptor activation is caused by a change in the local secondary structure of the *neu** transmembrane domain in the region of position 664. Brandt-Rauf *et al.*⁹ found that the minimum-energy conformation of *neu* contains a sharp bend at positions 664 and 665, while the corresponding region of the oncogenic *neu** sequence is α -helical.

In this paper, the first steps are taken towards high-resolution structures of the neu (Val 664) and neu* (Glu 664) transmembrane sequences. Since the structure of the single-pass transmembrane domain of neu* is likely to be sensitive to its membrane environment, structural measurements are made in lipid bilayers or multilayers. This rules out the traditional high-resolution structural methods of X-ray diffraction and solution NMR which cannot be applied to the study of proteins embedded in membrane bilayers. The approach we have taken involves a combination of polarized IR and magic angle spinning NMR spectroscopy^{10,11}. Polarized IR measurements are used to define the global secondary structure and orientation of the neu and neu* transmembrane domains, and magic angle spinning NMR measurements are used to establish the protonation state and strength of the hydrogen-bonding interactions involving the Glu 664 δ -carboxyl group. These studies provide the first direct structural data on the role of Glu 664 and membrane surface charge in the mechanism of receptor dimerization and activation.

Secondary structure and orientation of the neu and neu* transmembrane sequences

The global secondary structure of membrane proteins and peptides can be probed using polarized FTIR spectroscopy¹². The amide I vibration, composed predominantly of the backbone C=O stretching coordinate, is sensitive to protein secondary structure¹³. The frequency of the amide I mode depends on hydrogen-bonding of the C=O group and the geometry of the peptide backbone atoms. Bands centred at $\sim 1655\text{ cm}^{-1}$ correspond to α -helical structures, while bands centred at ~ 1624 – 1637 cm^{-1} and 1675 – 1695 cm^{-1} correspond to the out-of-phase and in-phase modes of β -structure, respectively^{14–16}. Side-chain vibrations from the amido, amino and guanidino groups of glutamine, lysine and arginine also contribute intensity in the 1600 – 1700 cm^{-1} amide I window¹⁷ and typically represent 15–20% of the total intensity in this region¹².

Measurements were performed on 38-residue neu and neu* transmembrane peptides (corresponding to residues 649–686 of the full length receptor). We first investigated the global secondary structure of the neu (Val 664) transmembrane sequence. The neu peptide incorporated into dimyristoylphosphatidylcholine (DMPC) bilayers at pH 7.0 is almost entirely helical. The amide I band is observed at 1655 cm^{-1} in polarized attenuated total reflection (ATR)-FTIR spectra (Fig. 1), characteristic of helical secondary structure. Fourier self-deconvolution (FSD) enhances the resolution of the frequency components in the amide I envelope¹⁸ and clearly shows the absence of other secondary structural elements. The residual intensity observed in the FSD spectrum ($\sim 15\%$ of the total intensity) can in large part be attributed to the side-chain vibrations of arginine, lysine and glutamine residues present in the neu transmembrane sequence. There are four arginines, two lysines and one glutamine in the transmembrane neu peptides which are estimated to represent $\sim 11\%$ of the total intensity between 1600 – 1700 cm^{-1} based on the bandwidths and

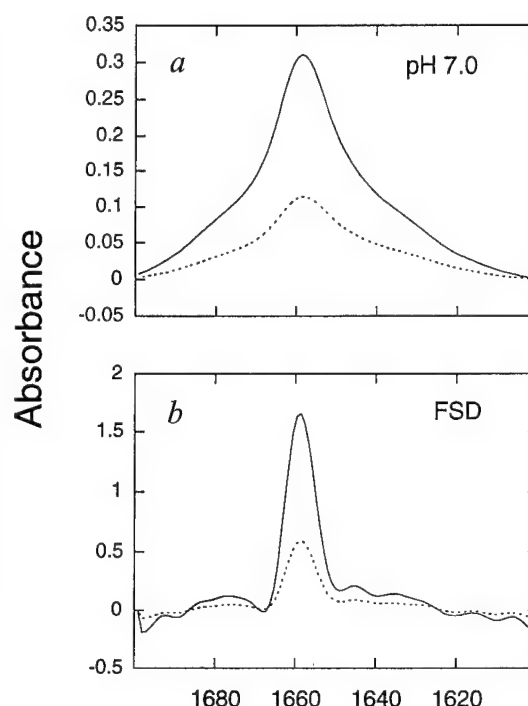


Fig. 1 Polarized ATR-FTIR spectra of the amide I band of a, neu (Val 664) along with b, its Fourier self-deconvolution. Spectra were obtained of the neu transmembrane domain incorporated into DMPC multilayers at pH 7.0 using parallel (solid lines) and perpendicularly (dashed lines) polarized light.

extinction coefficients previously reported for amino-acid side chain and peptide backbone vibrations^{15–17}.

Polarized IR spectra of the neu* (Glu 664) peptide incorporated into DMPC bilayers at pH 7.0 are quite different from those of neu (Val 664). The FSD spectrum of neu* at pH 7.0 (Fig. 2b) shows that in addition to a helical component at 1655 cm^{-1} , there is an intense band at 1630 cm^{-1} attributed to extended β -structure. We found that decreasing the pH to 5.5 (Fig. 2a) eliminates the 1630 cm^{-1} component and that α -helix again dominates the transmembrane secondary structure. Quantitation of the deconvoluted transmission IR spectrum (data not shown) indicates that the neu* transmembrane peptide at pH 5.5 in DMPC is $80\% \pm 5\%$ α -helix.

The orientation of the transmembrane helices in neu and neu* can be determined from the relative absorption of polarized IR light (see Methods). The neu helix is oriented at an angle of 20 – 25° relative to the bilayer normal based on the dichroic ratio (A_{\parallel}/A_{\perp}) of the 1655 cm^{-1} FSD band (see Methods). The orientation of the neu* helix in DMPC is slightly less perpendicular to the membrane plane than observed for neu. The average helix tilt angle of the neu* peptide calculated from the series of polarized FTIR spectra (Figs 2a–c) obtained in DMPC is 30 – 35° . However, the orientation of the neu* helix improves when dimyristoylphosphatidylserine (DMPS) is incorporated into the DMPC bilayers (Figs 2d–f, see below) and is comparable to that observed for neu. An orientation of

20–25° is in the range calculated for transmembrane helices that pack together in a left-handed coiled-coil geometry^{19,20}.

The most straightforward interpretation of these data is that increasing the pH results in local unfolding of the peptide. Our hypothesis is that protonation of Glu 664 allows the peptide to fold into a long α -helix that spans the membrane and extends from the C terminus through position 664. Deprotonation leads to unfolding of the helix from Glu 664 to the N terminus of the protein. This suggests that Glu 664 titrates with a pK_a between 5.5 and 7, a substantial increase over the 4–4.5 pK_a of glutamic acid in solution. An increase in the apparent pK_a of carboxylic acid groups in membrane lipids and fatty acids has previously been observed in negatively charged membrane vesicles due to an increase in surface pH^{21–23}. The large observed shift in pK_a is significant considering that the phosphatidylcholine headgroup of DMPC is neutral. One test of this hypothesis would be the observation of a frequency shift of the COOH vibration on deprotonation. However, this vibration is obscured under the intense lipid acyl chain C=O vibration at $\sim 1735\text{ cm}^{-1}$ (data not shown). Characteristic frequency changes are observed in the $^{13}\text{COOH}$ NMR chemical shift (see below) providing direct evidence for COOH deprotonation.

Membrane surface charge shifts the pK_a of Glu 664

The effect of membrane surface charge on the pK_a of Glu 664 can be examined by both polarized IR and magic angle spinning NMR. In order to establish how membrane surface charge influences the carboxyl group pK_a , we made the membrane bilayers more negatively charged by incorporating DMPS into the DMPC vesicles at a mole ratio of 14%. DMPS is the

major negatively charged lipid in mammalian cell membranes and usually ranges in concentration from 10–20%. The influence on surface potential of 14% DMPS in host DMPC bilayers has been characterized by potentiometric titrations and surface potential measurements²². The apparent pK_a of 4.7 observed for the PS carboxyl group is shifted ~ 1 pH unit higher than its intrinsic pK_a of 3.6 in 10 mM NaCl. The FSDs of the neu* transmembrane peptide in DMPC:DMPS membranes are shown in Figs 2d–f. In contrast to the behaviour seen in DMPC bilayers, only a single 1655 cm^{-1} resonance is observed in the DMPC:DMPS bilayers up to pH 8.5. The FSDs of polarized IR spectra obtained at pH 9.5–11 exhibit a band at 1630 cm^{-1} similar to that seen for DMPC membranes between pH 7–8.5 (data not shown) suggesting that the pK_a of Glu 664 has shifted to between 8.5 and 9. Finally, the frequency and intensity of the amide I band at 1655 cm^{-1} obtained from transmission spectra argue that the peptide is 80–90% helical below pH 8.5, corresponding to 30–34 residues of the 38 residue neu* peptide. Since only 14–18 amino acids are needed to span the bilayer²⁴, the transmembrane helix must extend through the membrane interface.

The pK_a of the Glu 664 side chain of neu* in membrane bilayers can also be established using magic angle spinning (MAS) NMR. The isotropic ^{13}C chemical shift of the glutamate carboxyl group is sensitive to its protonation state and characteristically shifts upfield upon protonation²⁵. The frequency of the $^{13}\text{COOH}$ NMR resonance can readily be followed by obtaining spectra of the neu* transmembrane peptide that has been specifically labelled with ^{13}C at the Glu 664 carboxyl group.

Fig. 3 presents MAS NMR spectra of the neu* transmembrane sequence in DMPC bilayers at pH 5.5 (a), pH 7.0 (b) and pH 8.5 (c). In Fig. 3a, the resonance at 179.5 p.p.m. is assigned to the side chain carboxyl of Glu 664 based on a comparison with unlabelled peptide. Increasing the pH to 7.0 (Fig. 3b) results in the appearance of a second resonance at 180.7 p.p.m. The intensity of the 180.7 p.p.m. resonance increases when the pH is raised to pH 8.5 (Fig. 3c).

Integration of the intensities of a pH series from pH 5.5–8.5 indicates that the apparent pK_a of Glu 664 in DMPC bilayers is ~ 6.5 (Fig. 4). This represents a substantial shift (~ 2 pH units) from the intrinsic pK_a of glutamate. A pK_a of 6.5 indicates that the Glu 664 side chain is still charged at physiological pH and unable to partition into the membrane. A further increase in the pK_a , however, is observed for neu* in DMPC:DMPS membranes which bear a net negative surface charge. The MAS NMR measurements of 5- ^{13}C -Glu 664 neu* in DMPC:DMPS membranes correlate with the FTIR results and show that the pK_a shifts to ~ 9 . The large shift in the pK_a of the Glu 664 carboxyl group relative to the carboxyl group in the phosphatidylserine headgroup in DMPS may reflect stabilization of the protonated Glu 664 side chain due to dimerization.

One important note in comparing the NMR and IR data is the close agreement of the estimated pK_a even though the sample conditions are quite different. The NMR data were obtained of hydrated membranes at

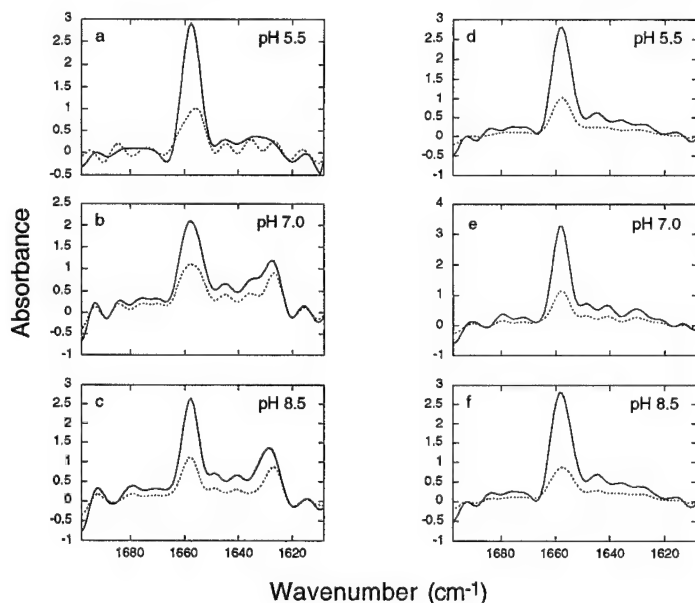


Fig. 2 Fourier self-deconvolutions of the amide I band of neu* (Glu 664). Spectra were obtained of neu*TM incorporated in a–c, DMPC or d–f, DMPC:DMPS multilayers at pH 5.5, pH 7.0 and pH 8.5 using parallel (solid lines) and perpendicularly (dashed lines) polarized light.

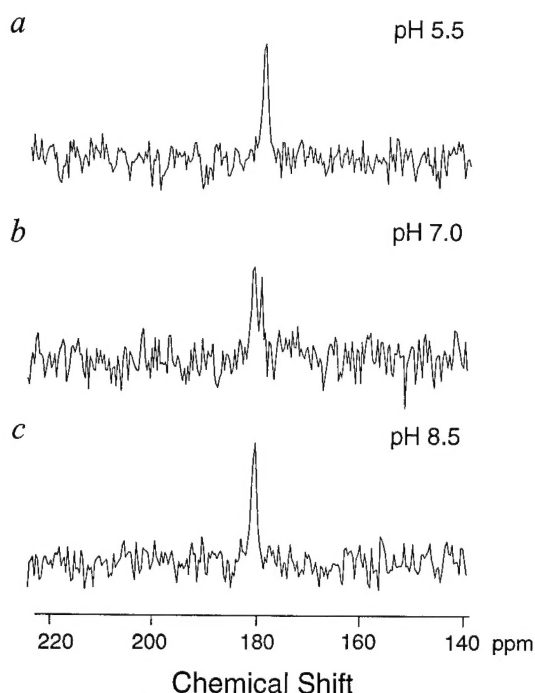


Fig. 3 MAS NMR spectra of neu* transmembrane domain at a, pH 5.5, b, pH 7.0 and c, pH 8.5 in DMPC multilayers. Spectra were obtained at a ^{13}C frequency of 90.4 MHz with a MAS speed of 5.0 kHz. Shown are the difference spectra where a spectrum of unlabelled neu* peptide reconstituted in DMPC has been subtracted. The temperature was maintained at -25°C . At higher temperatures, the two resonances broaden and collapse into a single line due to exchange.

low temperature. The IR data were obtained of dried films where the pH values indicated are those of the bulk solvent before depositing the film. This is necessary due to the strong IR absorption of water in the amide I region of the spectrum. It may be expected that the local pH increases substantially as the membranes are concentrated on the IR window. However, since only the bilayers in contact with the ATR germanium crystal are observed in the polarized IR experiment, one possibility for the absence of a large local pH change is that the membranes are layered (and solvent largely excluded) before the excess bulk solvent is evaporated.

Strong hydrogen bonding of Glu 664

The strength of hydrogen bonds formed by the Glu 664 δ -carboxyl group can be determined from the principal elements of the ^{13}C chemical shift tensor. The principal tensor elements (σ_{11} , σ_{22} and σ_{33}) can be calculated from the integrated intensities of the rotational side bands observed in a MAS NMR spectrum obtained at low spinning speeds²⁶. Based on an extensive series of model compounds, McDermott and co-workers found a strong correlation between the σ_{22} element of the chemical shift tensor and the O–H hydrogen-bonding distance between the carbonyl of a protonated acid and its nearest proton donor²⁵. Strong hydrogen-bonding interactions between two carboxyl

groups correlated with σ_{22} values greater than ~ 170 p.p.m., while weak hydrogen-bonding interactions between a carboxyl group and a carbonyl or amide group correlated with σ_{22} values less than ~ 170 p.p.m. In contrast, the σ_{11} and σ_{33} elements are largely insensitive to hydrogen-bonding interactions.

In order to provide a comparison with the neu* transmembrane sequence, we first obtained a series of MAS NMR spectra of crystalline L-glutamic acid. The carboxyl groups in the crystal structure are strongly hydrogen bonded²⁷. Fig. 5a presents the MAS NMR spectrum of double ^{13}C -labelled glutamic acid using a MAS frequency of 2.5 kHz. The isotropic resonance of the side chain δ -carboxyl is observed at 178 p.p.m. and is flanked by rotational side bands spaced by the MAS frequency. The +1 and –1 side bands have roughly the same intensity. The σ_{22} tensor element derived from an analysis of side band intensities is at 174 p.p.m. (Table 1); this is the largest downfield σ_{22} shift observed for protonated carboxyl groups in an extensive series of model compounds²⁵. The backbone carboxyl resonance is at 176 p.p.m. The +1 side band is more intense than both the centre band and –1 side band and reflects an upfield shift of the σ_{22} element to 165 p.p.m. Smaller shifts are observed for the σ_{11} and σ_{33} elements.

Fig. 5b presents a difference MAS NMR spectrum between unlabelled neu* and 5- ^{13}C -Glu 664-labelled neu* obtained under the same conditions as above. The difference spectrum exhibits only the resonances resulting from the 5- ^{13}C -labelled carboxyl group. The –1 sideband appears to be slightly more intense than the +1 side band suggesting a downfield shift in the σ_{22} tensor element. Side-band analysis (Table 1) based on MAS spectra obtained at several MAS frequencies confirms this observation. The σ_{22} element shifts from 174 p.p.m. to ~ 183 p.p.m. indicating a stronger H-bonding interaction for the δ -carboxyl group compared to crystalline glutamic acid. Based on a linear correlation between σ_{22} and the O–H hydrogen bond distance²⁵, the 183 p.p.m. shift would correspond with a 1.5 Å O–H separation.

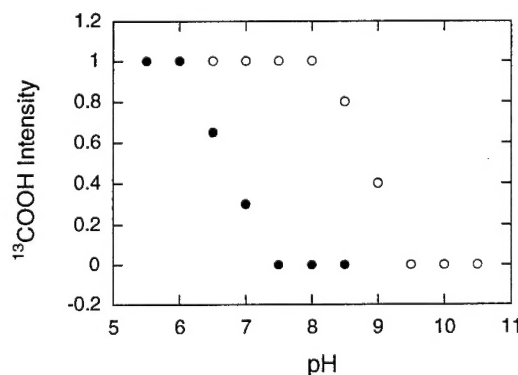


Fig. 4 Integrated intensity of the 5- ^{13}C -E664 resonance in the neu* transmembrane sequence as a function of pH. Titration curves are shown for the neu* peptide reconstituted into DMPC (●) and into DMPC:DMPS (○) multilayers.

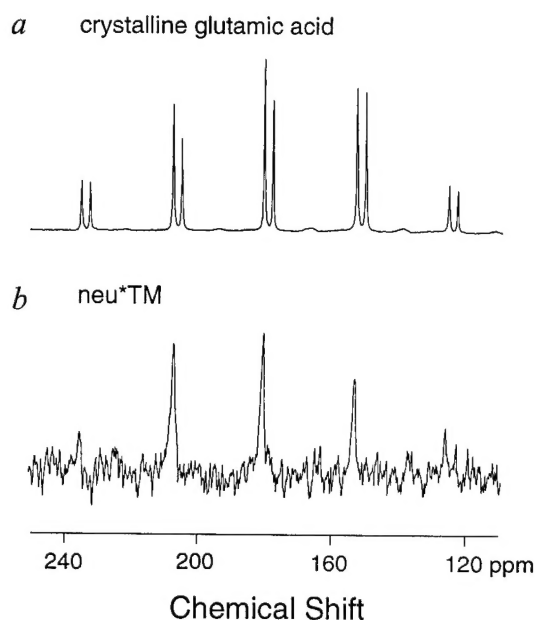


Fig. 5 MAS spectra of *a*, crystalline 1,5- ^{13}C glutamic acid and *b*, the neu* peptide in DMPC:DMPS membranes at pH 6.0. The MAS frequency was 2.5 kHz.

Structure of the neu* transmembrane domain

Fig. 6 presents a model that incorporates the results described above. First, the region C-terminal to position 664 is helical and oriented roughly perpendicular to the membrane plane. When the Glu 665 carboxyl group is deprotonated, the region N-terminal to position 664 unfolds and the COO^- group is exposed to the polar membrane interface. Protonation allows the peptide to adopt a helical conformation oriented perpendicular to the membrane plane. The pK_a of the Glu side chain is shifted by the membrane surface charge. Under conditions approximating those in native membranes, the carboxyl group readily protonates. It may partition into the membrane in a fashion similar to that of fatty acids which are observed to sink deeper into bilayers on protonation²⁸. The high pK_a of the Glu 664 carboxyl group, the large shift of the $^{13}\text{COOH}$ shift tensor and the increased perpendicular orientation of the transmembrane helix in DMPC:DMPS membranes suggest that the neu* transmembrane peptides dimerize in membranes.

What are the implications of these findings for the mechanism of receptor activation? First, the results do not support the model of Brandt-Rauf *et al.*⁹ that activation is caused by a change in secondary structure near position 664. Based on our data, the helical secondary structures of the neu and neu* transmembrane peptides are comparable once the Glu 664 carboxyl group is protonated in neu*. These are the first studies to directly address the structure of the neu and neu* transmembrane domains in membranes. Previous studies by Gullick *et al.*²⁹ on a much smaller fragment of the transmembrane domain reached a similar conclusion. However, in those studies several hydrophobic residues were replaced with serines to increase peptide solubility

and the measurements were made in trifluoroethanol rather than membrane bilayers. Further, the extremely strong hydrogen-bonding interactions and high pK_a of Glu 664 support models involving dimerization of the neu transmembrane domain in the activation mechanism. On the basis of the model compound studies of McDermott and co-workers²⁵, our data suggest that strong COOH-HOOC interactions occur in the dimer interface, although the COOH-O=C geometry predicted by Sternberg and Gullick cannot be ruled out. The COOH-HOOC geometry may be favoured since both carboxyl oxygens are able to participate in hydrogen bonding. However, one argument in support of the Sternberg-Gullick model is the observation that a short transmembrane sequence corresponding to the non-transforming neu (Val 664) protein is able to inhibit transformation when coexpressed with the neu* (Glu 664) protein³⁰. This would be possible if only a single glutamate in the helix interface is needed for dimerization. Direct internuclear distance measurements using MAS NMR methods can distinguish these two models.

The high pK_a of Glu 664 explains several other mutations made at residue 664. First, Bargmann and Weinberg have observed that glutamate and glutamine have the same high transforming potential^{3,4}. The high Glu 664 pK_a is consistent with this observation since the glutamine side chain can participate in the same hydrogen-bonding interactions as the glutamate COOH . The observation that lysine or histidine residues are not transforming makes sense in light of our data on pK_a shifts due to membrane surface charge. A negative membrane potential will have opposite effects on the pK_a of basic and acidic residues. The pK_a of basic residues will be lowered in negatively charged membranes leading to more stable charged species. Finally, the observation that substitution of aspartate at position 664 does not activate the rat receptor suggests that side chain length is important for bridging the helix interface and establishing strong hydrogen bonds.

Our results suggest that the AxxVG sequence motif recognized by Sternberg and Gullick may, in fact, represent a dimerization motif in the non-transforming receptor to orient the transmembrane helices upon ligand binding. This motif appears in many non-transforming growth factor receptors and would be expected to lie in the helix interface of the ligand-activated receptor based on the 'front-to-front' association of helices in neu*. Support for the idea that the AxxVG sequence may represent a dimerization motif comes from studies which show that the ectodomain may prevent dimerization without ligand⁴ in a manner sim-

Table 1 Principal chemical shift tensor values for glutamic acid¹ and neu* (Glu 664)²

Compound	Isotropic	σ_{11}	σ_{22}	σ_{33}
Glutamic Acid	176	256	165	106
Glutamic Acid - δ	178	252	174	109
neu*	179.5	251 \pm 4	183 \pm 3	105 \pm 2

¹Values from ref. 25 and reproduced in this study.

²The chemical shift tensor elements of neu* were determined from measurements at MAS speeds of 3.0, 2.5 and 2.0 kHz.

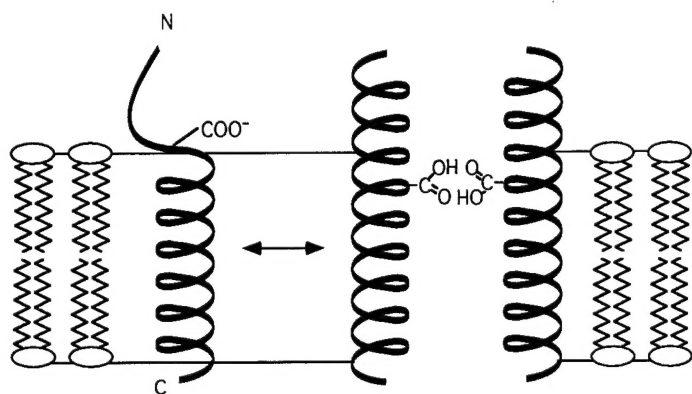


Fig. 6 Model illustrating the influence of membrane surface potential on the pK_a of Glu 664 in neu*. The Glu 664 carboxyl group is deprotonated and the sequence N-terminal to position 664 unfolds into extended β - or random coil structure when the pH is above the $COOH$ pK_a . Protonation allows the entire transmembrane peptide to adopt a helical conformation oriented perpendicular to the membrane plane. The pK_a of the Glu 664 side chain is shifted by the membrane surface charge up to a value of 8.5–9 in DMPC:DMPS membranes. This allows the carboxyl group to readily partition into the membrane. The high pK_a and the large downfield shift in the σ_{22} shift tensor element for the $^{13}COOH$ group argue that the neu* transmembrane peptides dimerize in membranes. Comparison of the chemical shifts observed in neu* and crystalline glutamic acid suggests that strong $COOH-HOOC$ interactions occur in the dimer interface.

ilar to that suggested for other growth factor receptors^{31–34}. In neu*, we propose that the strong hydrogen-bonding interaction generated by the V664E substitution overcomes the inhibition by the ectodomain and orients the transmembrane helices in an active geometry.

Methods

Synthesis and reconstitution. The neu and neu* transmembrane peptides were synthesized using solid-phase methods at the Keck Peptide Synthesis Facility at Yale University. N-t-BOC-5- ^{13}C -glutamic acid was obtained from Cambridge Isotopes (Andover, MA.) and 1,5- ^{13}C glutamic acid was obtained from the Stable Isotope Resource (Los Alamos, NM). The sequence of the neu* transmembrane peptide corresponds to residues 649–686 in the rat neu receptor protein (AEQRASPVTFIIATV-E664-GVLLFLILVVV-GILKRRRYK). The crude peptide was purified by reverse phase high performance liquid chromatography (RP-HPLC). The lyophilized peptide was dissolved in trifluoroacetic acid and injected on a semipreparative Vydac C4 column equilibrated with 50% H_2O , 20% acetonitrile and 30% 2-propanol. Peptide elution was achieved with a linear gradient to a final solvent composition of 40% acetonitrile and 60% 2-propanol. All solvents contained 0.1% trifluoroacetic acid. Fractions containing peptides were then lyophilized and assessed for purity by amino acid analysis (correlation coefficients of > 0.95) and mass spectrometry. It was found that peptides with the correct sequence eluted later than peptides that contained an amino-acid deletion.

Peptide fractions were lyophilized and reconstituted into lipids as follows. Peptide and lipids were dissolved together at a 30:1 molar ratio with 2% n-octyl β -glucopyranoside (Sigma, St. Louis, MO) in trifluoroethanol. The lipids (Avanti Polar Lipids, Alabaster, AL) we used were dimyristoyl phosphatidylcholine (DMPC) and dimyristoyl phosphatidylserine (DMPS). Samples were dried with nitrogen gas, resolubilized, and then divided into aliquots. Several different buffers were used to span the pH range from pH 5.5–11: MES (pH 5.5–6.7), HEPES (pH 6.8–8.2), TAPS (pH 7.7–9.1), CHES (pH 8.6–10) and CAPS (pH 9.7–11.1). Buffers contained

0.5 mM sodium azide and 10 mM NaCl. Samples were dialysed for 24–48 hours to remove n-octyl β -glucopyranoside using Spectra-Por 3 dialysis tubing (3,500 MW cutoff). The samples were then run on sucrose gradients (15–50%) to isolate homogeneous reconstituted vesicles and the sucrose was removed by dialysis. 300 μ l of each sample were allocated for ATR-FTIR. The remainder of the sample was pelleted for magic angle spinning NMR experiments.

FTIR spectroscopy. ATR-FTIR spectra were collected on a Nicolet Magna 550 spectrometer with a liquid nitrogen cooled detector. The sample chamber was purged with nitrogen, and the samples layered on a germanium crystal plate and dried using argon or nitrogen. Each spectrum represents the average of 1000 scans acquired at a resolution of 4 cm^{-1} using light polarized at either 0 or 90 degrees. The data was processed by automatic baseline correction, followed by Fourier self-deconvolution of the helix peak (~ 1655 cm^{-1}) using a bandwidth of 13 cm^{-1} , an enhancement of 2.4, and Happ-Genzel apodization^{18,20}.

The analysis of the dichroic ratio observed in the polarized ATR spectra follows the discussion of Harrick³⁵. The electric field amplitudes of the evanescent wave are given by:

$$E_x = 2(\sin^2\phi - n_2^2)^{1/2} \cos\phi / [(1 - n_2^2)^{1/2} \{ (1 + n_2^2) \sin^2\phi - n_2^2 \}^{1/2}]$$

$$E_y = 2 \cos\phi / (1 - n_2^2)$$

$$E_z = 2 \sin\phi \cos\phi / [(1 - n_2^2)^{1/2} \{ (1 + n_2^2) \sin^2\phi - n_2^2 \}^{1/2}]$$

where ϕ is the angle of incidence between the IR beam and the internal reflection element (45°), and n_2 is the ratio between the refractive indices of the sample ($n_2=1.43$) and the internal reflection element ($n_1=4.0$)^{36–38}. These equations are based on the assumption that the thickness of the deposited film (>20 nm) is much larger than the penetration depth (~ 1 mm) of the evanescent wave (see Ref. 35). The electric field components together with the dichroic ratio (defined as the ratio between absorption of parallel ($A_{||}$) and perpendicular (A_{\perp}) polarized light, $R^{ATR}=A_{||}/A_{\perp}$) are used to calculate an order parameter defined as:

$$S = 3/2 \langle \cos^2\theta \rangle - 1/2$$

with the following equation:

$$S = 2(E_x^2 - R^{ATR} E_y^2 + E_z^2) / [(3 \cos^2\alpha - 1)(E_x^2 - R^{ATR} E_y^2 - 2E_z^2)]$$

where θ is the angle between the helix director and the normal of the internal reflection element, and α is the angle between the helix director and the transition dipole moment of the amide I vibrational mode. Values for α in the literature range from $29-40^\circ$ ($29-34^\circ$ (ref. 39), 40° (Ref. 40); 39° (ref. 41)). For the calculations in this study, we have assumed an average value of 39° .

NMR spectroscopy. Magic angle spinning NMR experiments were performed on a Chemagnetics CMX 360 MHz spectrometer using a 5 mm high-speed probe from Doty Scientific (Columbia, SC). The crystalline glutamic acid samples were prepared by crystallizing 1,5- ^{13}C glutamic acid from a concentrated HCl solution²⁷. The reconstituted neu samples were prepared by pelleting membrane vesicles at $80,000 \times g$ in an ultracentrifuge and loading the hydrated pellets into the NMR rotor. The sample spinning speed was kept constant to within 5 Hz and the sample temperature was maintained at $-25^\circ C$. Spectra were obtained with a standard cross polarization pulse sequence using a 4 ms proton 90° pulse, 2 ms cross polarization pulses, a 33 ms acquisition time and a 3 s recycle delay for the neu samples and a 10 s recycle delay for the crystalline glutamate samples. Typically, 10,000–20,000 transients were averaged for each spectrum.

Received 14 September 1995; accepted 11 January 1996.

Acknowledgements

We thank M. Groesbeek, K. Aschheim and M. Zilio for technical assistance, and D. Stern, D. Engelman, A. Brünger and V. Rath for critical comments on the manuscript. The $1,5\text{-}^{13}\text{C}$ glutamic acid was kindly provided by the Stable Isotope Resource at Los Alamos. This work was supported by a grant from the Department of the Army, Medical Research.

- Schlessinger, J. & Ulrich, A. Growth factor signalling by receptor tyrosine kinases. *Neuron* **9**, 383–391 (1992).
- Hynes, N.E. & Stern, D.F. The biology of erbB-2/neu/HER-2 and its role in cancer. *Biochim. Biophys. Acta* **1198**, 165–184 (1994).
- Bargmann, C.I., Hung, M.-C. & Weinberg, R.A. Multiple independent activations of the neu oncogene by a point mutation altering the transmembrane domain of p185. *Cell* **45**, 649–657 (1986).
- Bargmann, C.I. & Weinberg, R.A. Oncogenic activation of the neu-encoded receptor protein by point mutation and deletion. *EMBO J.* **7**, 2043–2052 (1988).
- Cao, H., Bangalore, L., Bormann, B.J. & Stern, D.F. A subdomain in the transmembrane domain is necessary for p185neu* activation. *EMBO J.* **11**, 923–932 (1992).
- Cao, H., Bangalore, L., Dompe, C., Bormann, B.J. & Stern, D.F. An extra cysteine proximal to the transmembrane domain induces differential crosslinking of p185neu and p185neu*. *J. Biol. Chem.* **267**, 20489–20492 (1992).
- Sternberg, M.J. & Gullick, W.J. Neu receptor dimerization. *Nature* **339**, 587 (1989).
- Sternberg M.J.E. & Gullick, W.J. A sequence motif in the transmembrane region of growth factor receptors with tyrosine kinase activity mediates dimerization. *Protein Eng.* **3**, 245–248 (1990).
- Brandt-Rauf, P.W., Rackovsky, S. & Pincus, M.R. Correlation of the structure of the transmembrane domain of the neu oncogene-encoded p185 protein with its function. *Proc. Natl. Acad. Sci. USA* **87**, 8660–8664 (1990).
- Smith, S.O., Jonas, R., Braiman, M.S. & Bormann, B.J. Structure and orientation of the transmembrane domain of glycophorin A in lipid bilayers. *Biochemistry* **33**, 633–641 (1994).
- Smith, S.O. & Bormann, B.J. Determination of helix-helix interactions in membranes by rotational resonance NMR. *Proc. Natl. Acad. Sci. USA* **92**, 488–491 (1995).
- Surewicz, W.K., Mantsch, H.H. & Chapman, D. Determination of protein secondary structure by fourier transform infrared spectroscopy: a critical assessment. *Biochemistry* **32**, 389–394 (1993).
- Braiman, M.S. & Rothschild, K.J. Fourier transform infrared techniques for probing membrane protein structure. *Annu. Rev. Biophys. Biophys. Chem.* **17**, 541–570 (1989).
- Byler, M.D. & Susi, H. Examination of the secondary structure of proteins by Deconvolved FTIR spectra. *Biopolymers* **25**, 469–487 (1986).
- Veniaminov, S.U. & Kalnin, N.N. Quantitative IR spectroscopy of peptide compounds in water (H₂O) solutions. II. Amide absorption bands of polypeptides and fibrous proteins in α -, β -, and random coil conformations. *Biopolymers* **30**, 1259–1271 (1990).
- Veniaminov, S.U. & Kalnin, N.N. Quantitative IR spectrophotometry of peptide compounds in water (H₂O) solutions. III. Estimation of the protein secondary structure. *Biopolymers* **30**, 1273–1280 (1990).
- Veniaminov, S.U. & Kalnin, N.N. Quantitative IR spectroscopy of peptide compounds in water (H₂O) solutions. I. Spectral parameters of amino acid residue absorption bands. *Biopolymers* **30**, 1243–1257 (1990).
- Kauppinen, J.K., Moffatt, D.J., Mantsch, H.H. & Cameron, D.G. Fourier self-deconvolution: a method for resolving intrinsically overlapped bands. *Appl. Spectrosc.* **35**, 271–276 (1981).
- Chothia, C., Levitt, M. & Richardson, D. Helix-to-helix packing in proteins. *J. Mol. Biol.* **145**, 215–250 (1981).
- Arkin, I.T., Rothman, M., Ludlam, C.F.C., Aimoto, S., Engelman, D.M., Rothschild, K.J. & Smith, S.O. Structural model of the phospholamban ion channel complex in phospholipid membranes. *J. Mol. Biol.* **248**, 824–834 (1995).
- Kantor, H.L. & Prestegard, J.P. Fusion of phosphatidylcholine bilayer vesicles: role of free fatty acid. *Biochemistry* **17**, 3592–3597 (1978).
- Tsui, F.C., Ojcius, D.M. & Hubbell, W.L. The intrinsic pKa values for phosphatidylserine and phosphatidylethanolamine in phosphatidylcholine host bilayers. *Biophys. J.* **49**, 459–468 (1986).
- Ptak, M., Egret-Charlier, M., Sanson, A. & Bouloussa, O. A NMR study of the ionization of fatty acids, fatty amines and N-acylamino acids incorporated in phosphatidylcholine vesicles. *Biochim. Biophys. Acta* **600**, 387–397 (1980).
- Adams, G.A. & Rose, J.K. Structural requirements of a membrane-spanning domain for protein anchoring and cell surface transport. *Cell* **41**, 1007–1015 (1985).
- Gu, Z., Zambrano, R. & McDermott, A. Hydrogen bonding of carboxyl groups in solid-state amino acids and peptides: comparison of carbon chemical shielding, infrared frequencies, and structures. *J. Am. Chem. Soc.* **116**, 6368–6372 (1994).
- Herzfeld, J. & Berger, A.E. Side band intensities in NMR spectra of samples spinning at the magic angle. *J. Chem. Phys.* **73**, 6021–6030 (1980).
- Sequeira, A., Rajagopal, H. & Chidambaram, R. A neutron diffraction study of the structure of L-glutamic acid.HCl. *Acta Crystallogr.* **B28**, 2514–2519 (1972).
- Miyazaki, J., Hideg, K. & Marsh, D. Interfacial ionization and partitioning of membrane-bound local anaesthetics. *Biochim. Biophys. Acta* **1103**, 62–68 (1992).
- Gullick, W.J. *et al.* Three dimensional structure of the transmembrane region of the proto-oncogenic and oncogenic forms of the neu protein. *EMBO J.* **11**, 43–48 (1992).
- Lofts, F.J., Hurst, H.C., Sternberg, M.J.E. & Gullick, W.J. Specific short transmembrane sequences can inhibit transformation by the mutant neu growth factor receptor *in vitro* and *in vivo*. *Oncogene* **8**, 2813–2820 (1993).
- Downward, J. *et al.* Close similarity of epidermal growth factor receptor and v-erb-B oncogene protein sequences. *Nature* **307**, 521–527 (1984).
- Birchmeier, C., Birnbaum, D., Waitches, G., Fasano, O. & Wigler, M. Characterization of an activated human ros gene. *Mol. Cell Biol.* **6**, 3109–3116 (1986).
- Gamett, D.C., Tracey, S.E. & Robinson, H.L. Differences in sequences encoding the carboxyl-terminal domain of the epidermal growth factor receptor correlate with differences in disease potential of viral erbB genes. *Proc. Natl. Acad. Sci. USA* **83**, 6053–6057 (1986).
- Neckameyer, W.S., Shibuya, M., Hsu, M.-T. & Wang, L.-H. Proto-oncogene c-ros codes for a molecule with structural features common to those of growth factor receptors and displays tissue-specific and developmentally regulated expression. *Mol. Cell Biol.* **6**, 1478–1486 (1986).
- Harrick, N.J. *Internal reflection spectroscopy*. Interscience Publishers, New York (1967).
- Wolfe, W.F. & Zissis, G.J. in *The Infrared Handbook* (U.S. Government Printing Office, Washington 1978).
- Fringeli, U.P., Apell, H.J., Fringeli, M. & Lauger, P. Polarized infrared absorption of Na⁺/K⁺-ATPase studied by attenuated total reflection spectroscopy. *Biochim. Biophys. Acta* **984**, 301–312 (1989).
- Tamm, L.K. & Tatulian, S.A. Orientation of functional and nonfunctional PTS permease signal sequences in lipid bilayers. A polarized attenuated total reflection infrared study. *Biochemistry* **32**, 7720–7726 (1993).
- Miyazawa, T. & Blout, E.R. The infrared spectra of polypeptides in various conformations: amide I and amide II bands. *J. Am. Chem. Soc.* **83**, 712–719 (1961).
- Bradbury, E.M. *et al.* The structure of the ω -form of poly- β -benzyl-L-aspartate. *J. Mol. Biol.* **5**, 230–247 (1962).
- Tsuboi M. Infrared dichroism and molecular conformation of α -form poly- γ -benzyl-L-glutamate. *J. Polymer Sci.* **59**, 139–153 (1994).